the transmembrane region (PHAT matrix element difference = −6), and probable functional effects of Arg393Trp (*7) (PSIC score difference = 3.053), Tyr401Cys (*8) (3.382) and Asp786Glu (*9) (2.277), but no functional effects of *3 (1.446) and *5 (0.326).

In conclusion, the current study provided detailed information on *ABCC2* variations and haplotype structures in Japanese and also suggested a large ethnic difference in the frequencies of 3972C>T(Ile1324Ile) and 1446C>G (Thr482Thr) and their related haplotypes between Asians and Caucasians. This information would be useful for studies investigating the clinical significance of *ABCC2* alleles and haplotypes.

Acknowledgements: The authors thank Ms. Chie Sudo for her secretarial assistance.

References

1) Jedlitschky, G., Hoffmann, U. and Kroemer, H. K.: Structure and function of the MRP2 (ABCC2) protein and its role in drug disposition. *Expert Opin. Drug Metab. Toxicol.*, **2**: 351–66 (2006).
2) Wada, M.: Single nucleotide polymorphisms in *ABCC2* and *ABCB1* genes and their clinical impact in physiology and drug response. *Cancer Lett.*, **234**: 40–50 (2006).
3) Huang, Y.: Pharmacogenetics/genomics of membrane transporters in cancer chemotherapy. *Cancer Metastasis Rev.*, **26**: 183–201 (2007).
4) Taniguchi, K., Wada, M., Kohno, K., Nakamura, T., Kawabe, T., Kawakami, M., Kagotani, K., Okumura, K., Akiyama, S. and Kuwano, M.: A human canalicular multispecific organic anion transporter (cMOAT) gene is overexpressed in cisplatin-resistant human cancer cell lines with decreased drug accumulation. *Cancer Res.*, **56**: 4124–4129 (1996).
5) Hinoshita, E., Uchiumi, T., Taguchi, K., Kinukawa, N., Tsuneyoshi, M., Maehara, Y., Sugimachi, K. and Kuwano, M.: Increased expression of an ATP-binding cassette superfamily transporter, multidrug resistance protein 2, in human colorectal carcinomas. *Clin. Cancer Res.*, **6**: 2401–2407 (2000).
6) Cui, Y., Konig, J., Buchholz, J.K., Spring, H., Leier, I. and Keppler, D.: Drug resistance and ATP-dependent conjugate transport mediated by the apical multidrug resistance protein, MRP2, permanently expressed in human and canine cells. *Mol. Pharmacol.*, **55**: 929–937 (1999).
7) Wada, M., Toh, S., Taniguchi, K., Nakamura, T., Uchiumi, T., Kohno, K., Yoshida, I., Kimura, A., Sakisaka, S., Adachi, Y. and Kuwano, M.: Mutations in the canilicular multispecific organic anion transporter (cMOAT) gene, a novel ABC transporter, in patients with hyperbilirubinemia II/Dubin-Johnson syndrome. *Hum. Mol. Genet.*, **7**: 203–207 (1998).
8) Choi, J. H., Ahn, B. M., Yi, J., Lee, J. H., Lee, J. H., Nam, S. W., Chon, C. Y., Han, K. H., Ahn, S. H., Jang, I. J., Cho, J. Y., Suh, Y., Cho, M. O., Lee, J. E., Kim, K. H. and Lee, M. G.: MRP2 haplotypes confer differential susceptibility to toxic liver injury. *Pharmacogenet. Genomics*, **17**: 403–415 (2007).
9) Daly, A. K., Aithal, G. P., Leathart, J. B., Swainsbury, R. A., Dang, T. S. and Day, C. P.: Genetic susceptibility to diclofenac-induced hepatotoxicity: contribution of UGT2B7, CYP2C8, and ABCC2 genotypes. *Gastroenterology*, **132**: 272–281 (2007).
10) de Jong, F. A., Scott-Horton, T. J., Kroetz, D. L., McLeod, H. L., Friberg, L. E., Mathijssen, R. H., Verweij, J., Marsh, S. and Sparreboom, A.: Irinotecan-induced diarrhea: functional significance of the polymorphic ABCC2 transporter protein. *Clin. Pharmacol. Ther.*, **81**: 42–49 (2007).
11) Haenisch, S., Zimmermann, U., Dazert, E., Wruck, C. J., Dazert, P., Siegmund, S., Kroemer, H. K., Warzok, R. W. and Cascorbi, I.: Influence of polymorphisms of ABCB1 and ABCC2 on mRNA and protein expression in normal and cancerous kidney cortex. *Pharmacogenomics J.*, **7**: 56–65 (2007).
12) Han, J. Y., Lim, H. S., Yoo, Y. K., Shin, E. S., Park, Y. H., Lee, S. Y., Lee, J. E., Lee, D. H., Kim, H. T. and Lee, J. S.: Associations of ABCB1, ABCC2, and ABCG2 polymorphisms with irinotecan-pharmacokinetics and clinical outcome in patients with advanced non-small cell lung cancer. *Cancer*, **110**: 138–147 (2007).
13) Innocenti, F., Undevia, S. D., Chen, P. X., Das, S., Ramirez, J., Dolan, M. E., Relling, M. V., Kroetz, D. L. and Ratain, M. J.: Pharmacogenetic analysis of interindividual irinotecan (CPT-11) pharmacokinetic (PK) variability: Evidence for a functional variant of ABCC2. *2004 ASCO Annual Meeting Proceedings (Post-Meeting Edition).* Vol. 22, No. 14S (July 15 Supplement), 2004: Abstract No: 2010.
14) Naesens, M., Kuypers, D. R., Verbeke, K. and Vanrenterghem, Y.: Multidrug resistance protein 2 genetic polymorphisms influence mycophenolic acid exposure in renal allograft recipients. *Transplantation*, **82**: 1074–1084 (2006).
15) Rau, T., Erney, B., Gores, R., Eschenhagen, T., Beck, J. and Langer, T.: High-dose methotrexate in pediatric acute lymphoblastic leukemia: impact of ABCC2 polymorphisms on plasma concentrations. *Clin. Pharmacol. Ther.*, **80**: 468–476 (2006).
16) Zhou, Q., Sparreboom, A., Tan, E. H., Cheung, Y. B., Lee, A., Poon, D., Lee, E. J. and Chowbay, B.: Pharmacogenetic profiling across the irinotecan pathway in Asian patients with cancer. *Br. J. Clin. Pharmacol.*, **59**: 415–424 (2005).
17) Niemi, M, Arnold, K. A., Backman, J. T., Pasanen, M. K., Gödtel-Armbrust, U., Wojnowski, L., Zanger, U. M., Neuvonen, P. J., Eichelbaum, M., Kivisto, K. T. and Lang, T.: Association of genetic polymorphism in ABCC2 with hepatic multidrug resistance-associated protein 2 expression and pravastatin pharmacokinetics. *Pharmacogenet. Genomics.*, **16**: 801–808 (2006).
18) Itoda, M., Saito, Y., Soyama, A., Saeki, M., Murayama, N., Ishida, S., Sai, K., Nagano, M., Suzuki, H., Sugiyama, Y., Ozawa, S. and Sawada, J.: Polymorphisms in the *ABCC2* (cMOAT/MRP2) gene found in 72 established cell lines derived from Japanese individuals: an association between single nucleotide polymorphisms in the 5′-untranslated region and exon 28. *Drug Metab. Dispos.*, **30**: 363–364 (2002).
19) Kitamura, Y., Moriguchi, M., Kaneko, H., Morisaki, H., Morisaki, T., Toyama, K. and Kamatani, N.: Determination of probability distribution of diplotype configuration (diplotype distribution) for each subject from genotypic data using the EM algorithm. *Ann. Hum. Genet.*, **66**: 183–193 (2002).
20) Ito, S., Ieiri, I., Tanabe, M., Suzuki, A., Higuchi, S. and Otsubo, K.: Polymorphism of the ABC transporter genes, MDR1, MRP1 and MRP2/cMOAT, in healthy Japanese subjects. *Pharmacogenetics*, **11**: 175–184 (2001).
21) Bosch, T. M., Doodeman, V. D., Smits, P. H., Meijerman, I., Schellens, J. H. and Beijnen, J. H.: Pharmacogenetic screening

for polymorphisms in drug-metabolizing enzymes and drug transporters in a Dutch population. *Mol. Diagn. Ther.*, **10**: 175–185 (2006).

22) Nebert, D. W.: Suggestions for the nomenclature of human alleles: relevance to ecogenetics, pharmacogenetics and molecular epidemiology. *Pharmacogenetics*, **10**: 279–290 (2000).

23) Hirouchi, M., Suzuki, H., Itoda, M., Ozawa, S., Sawada, J., Ieiri, I., Ohtsubo, K. and Sugiyama, Y.: Characterization of the cellular localization, expression level, and function of SNP variants of MRP2/ABCC2. *Pharm. Res.*, **21**: 742–748 (2004).

24) Meyer zu Schwabedissen, H. E., Jedlitschky, G., Gratz, M., Haenisch, S., Linnemann, K., Fusch, C., Cascorbi, I. and Kroemer, H. K.: Variable expression of MRP2 (ABCC2) in human placenta: influence of gestational age and cellular differentiation. *Drug Metab. Dispos.*, **33**: 896–904 (2005).

25) Izzedine, H., Hulot, J. S., Villard, E., Goyenvalle, C., Dominguez, S., Ghosn, J., Valantin, M. A., Lechat, P. and Deray, A. G.: Association between *ABCC2* gene haplotypes and tenofovir-induced proximal tubulopathy. *J. Infect. Dis.*, **194**: 1481–1491 (2006).

26) Saito, S., Iida, A., Sekine, A., Miura, Y., Ogawa, C., Kawauchi, S., Higuchi, S. and Nakamura, Y.: Identification of 779 genetic variations in eight genes encoding members of the ATP-binding cassette, subfamily C (ABCC/MRP/CFTR. *J. Hum. Genet.*, **47**: 147–171 (2002).

GFP image analysis in the mouse orthotopic bladder cancer model

MARCO A. DE VELASCO[1], MOTOYOSHI TANAKA[1], SATOSHI ANAI[3], ATSUSHI TOMIOKA[3], KAZUTO NISHIO[2] and HIROTSUGU UEMURA[1]

Departments of [1]Urology and [2]Genome Biology, Kinki University School of Medicine, 377-2 Ohno-Higashi, Osaka-Sayama, Osaka; [3]Department of Urology, Nara Medical University, 840 Shijo-cho, Kashihara, Nara, Japan

Abstract. Precise and objective measurements of tumor response have yet to be standardized in the mouse orthotopic bladder cancer model. In this study, we used image analysis and green fluorescent protein (GFP) to objectively measure tumor size in response to chemotherapy. KU-7 human bladder cancer cells transfected with GFP were intravesically inoculated into 8-week-old female nude mice. Fourteen days after tumor cell inoculation, the mice were assigned into a control (PBS) group or a doxorubicin (conc. 1.0 mg/ml) treatment group and received a single instillation of treatment. Fourteen days after treatment, the bladders were surgically exposed and fluorescent images were captured and later analyzed using image analysis. Bladders were processed for histological examination. Tumor incidence determined by GFP expression and histology was 100 and 80%, respectively, in the doxorubicin treatment group. A 9-fold (histology) vs. 12-fold (GFP expression) difference in tumor regression measured by tumor area ($P<0.05$) and a 5-fold (histology) vs. 9-fold (GFP expression) difference in tumor regression measured by the percent of tumor area in the bladder ($P<0.001$) were observed in the doxorubicin treatment group. Our findings suggest that using image analysis provides a precise, sensitive and objective means to measure tumor growth and treatment response in the mouse orthotopic bladder cancer model in lieu of histological methods. Consequently, the number of mice required in an experiment can be reduced since tissue samples are not needed for histology, thus making tissue samples readily available for additional assays in both a labor-effective and cost-effective manner.

Correspondence to: Dr Motoyoshi Tanaka, Department of Urology, Kinki University School of Medicine, 377-2 Ohno-Higashi, Osaka-Sayama, Osaka 589-8511, Japan
E-mail: mtanaka@med.kindai.ac.jp

Abbreviations: BCG, Bacille Calmette-Guérin; CCD, charge-coupled device; Dox, doxorubicin; EDTA, ethylenediamine tetra-acetic acid; GFP, green fluorescent protein; H&E, hematoxylin and eosin; PBS, phosphate-buffered saline; PSA, prostate specific antigen; ROI, region of interest

Key words: bladder cancer, green-fluorescent proteins, mouse, computer-assisted image analysis

Introduction

In the United States alone, urinary bladder cancer accounts for over 60,000 new cases per year and in Japan, over 16,000 new cases are reported annually (1,2). In Japan and western countries over 90% of the bladder carcinomas are urothelial carcinomas (3). Transurethral resection in combination with intravesical Bacille Calmette-Guérin (BCG) or chemotherapy are the mainstay for treatment of these lesions; however, 5- and 10-year recurrence rates of over 60 and 90%, respectively, pose a major challenge in the treatment and eradication of disease (3,4). These factors combined necessitate further evaluation of new treatment strategies.

Orthotopic tumor models provide researchers with an invaluable research tool, as tumor cells are able to grow in a native environment that more closely resembles its natural state. The mouse orthotopic bladder cancer model has been used for over 30 years, recently this model was modified by using human bladder cancer cells transfected with green fluorescent protein (GFP) implanted transurethally for *in vivo* visualization of tumor growth (5-7). GFP, a spontaneously fluorescent protein that absorbs UV-blue light and emits green fluorescence, has been shown to be suitable in monitoring and visualizing tumors *in vivo* (8). Additionally, tracking cells that stably express GFP *in vivo* allows for a rapid and more precise method for detecting tumor cells than the more traditional histological methods (9). Orthotopic bladder cancer models have already been used successfully to measure the treatment efficacy in chemotherapy, immunotherapy, gene therapy, and chemoprevention models (10-13). This system provides an ideal setting for testing chemotherapeutic agents *in vivo*; however, the challenge to accurately, practically, and objectively measure tumor response remains. Traditional means to measure tumor response have either been qualitative (rather than quantitative) or subjective. The use of computer assisted image analysis provides a solution to this problem in that it allows for a means to measure data in an unbiased manner. Measurement data can be spatially calibrated and since the manner of analysis is standardized, the results are consistently reproduced.

We propose a model that allows the use of image analysis software to accurately measure the growth and response of orthotopically implanted GFP-labeled human bladder cancer cells to intravesical drug treatment. For this purpose, we used doxorubicin (Dox), an anthracycline antibiotic commonly used in maintenance therapy for superficial bladder cancer (4).

Materials and methods

Bladder cancer cell line and transfection. KU-7, a human bladder cancer cell line derived from a superficial papillary tumor was used for our experiments (14). KU-7 cells were maintained in Gibco DMEM (Dulbecco's modified Eagle's medium) (Invitrogen, Carlsbad, CA) supplemented with 10% fetal calf serum in a 37˚C incubator with 5% CO_2. Stable GFP clones were generated as previously described (7). GFP expression was confirmed under a fluorescence microscope.

Orthotopic tumor implantation and intravesical treatment. Prior to bladder instillation, the cells were trypsinized and re-suspended in serum-free DMEM at a concentration of $1x10^8$ cells/ml. A method for the orthotopic instillation of tumor cells has been described (7). Briefly, eleven 8-week-old female athymic nude mice were anesthetized by intraperitoneal injection with Nembutal (Dainippon Sumitomo Pharma, Osaka, Japan). A 24-gauge catheter was inserted transurethrally into the bladder (Fig. 1A) and washed with 200 µl of PBS (phosphate-buffered saline). The bladder was emptied and 100 µl of 0.2% trypsin in 0.02 EDTA (Invitrogen, Carlsbad, CA) was infused and retained for 20 min. A 100-µl KU-7/GFP cell suspension containing $1x10^7$ cells was instilled into the bladder thereafter. The urethra was then ligated for 2-3 h with a purse-string suture to prevent leakage of tumor cells. Fourteen days after cell implantation, the animals were assigned to a control (PBS) (n=6) or doxorubicin (doxorubicin hydrochloride) (Kyowa Hakko Co. Ltd., Tokyo, Japan) (conc. 1.0 mg/ml) (n=5) treatment group and received a single intravesical treatment instillation that was retained for 1 h by purse-string suture.

In vivo fluorescence analysis of mouse bladders. Twenty-eight days following the instillation of tumor cells, the mice were again anesthetized as previously described and the bladders were surgically exposed. The whole mouse was placed under a Leica MZFL (FLVO III) dissecting stereomicroscope equipped with a fluorescent light source with a GFP2 filter and a CCD camera (Leica Microsystems, Heerbrugg, Switzerland). The exposed bladders were examined under fluorescence for the presence of tumors and digital images were captured under both fluorescent and incandescent light (Fig. 1B-D). The mice were then sacrificed and bladders were removed then fixed in 10% neutral buffered formalin.

Histological examination. The bladders were fixed overnight in 10% neutral buffered formalin and then transferred to 70% ethanol. Bladders were then sliced transversally in half and examined under a stereomicroscope. Tumor presence was confirmed and representative images were captured. The samples were then embedded in paraffin, step-sectioned and stained with hematoxylin and eosin (H&E). Tumors were verified under a light microscope and representative digital images were recorded for subsequent image analysis.

Image analysis. Image analysis was performed with ImageJ public domain software available through the National Institutes of Health (Bethesda, MD; available at http://rsb.info.nih.gov/ij/). All images were spatially calibrated for area measurements. Fig. 2 demonstrates an example of the process used to analyze and measure the bladders and tumors. Images of the processed bladders were captured from H&E stained slides and both the bladder and tumors were traced individually and identified by creating a ROI (region of interest) for each. The area was then calculated for each of the selected ROIs. Multiple step sections were taken from the embedded bladders and sections containing the largest tumor size were used for the area calculations. In cases with multiple tumors, lesions were identified and measured individually, however, the measurement data from multiple tumors in an individual bladder was pooled and the area is represented as a single area measurement.

Statistical analysis. Data were statistically analyzed using the Student's t-test and differences were considered to be significant at $P<0.05$. For comparisons between histological analysis and GFP expression, regression analysis was performed. Statistical analysis was carried out using SigmaStat 3.5 (Systat Software, Inc., Jose, CA).

Results

Tumor incidence. We first measured tumor incidence for the implanted KU-7/GFP cancer cells. To measure tumor incidence by GFP expression, surgically exposed bladders were viewed under blue fluorescent light. Bladders without tumors failed to demonstrate any fluorescence; on the other hand, bladders with tumors expressing GFP were easily identified by green fluorescence. Tumor appearance ranged from small individual nests of cells to multiple clusters and/or large masses (Fig. 3). Tumor incidence is defined as the percentage of mice with visible tumors and was determined by direct observation of positive GFP cells within the bladder *in vivo* and/or the presence of tumor cells in the bladder by histological examination. Tumor incidence measured by GFP expression was 100% for all mice in the control and doxorubicin groups. Tumor incidence measured by histological analysis was 100% for the control group but 80% for the doxorubicin treatment group. Histological analysis for tumor incidence failed to reveal microscopic lesions that were clearly detectable by GFP fluorescence.

Measurements of tumor area. Next, we confirmed that cells emitting the green fluorescence were indeed the KU-7/GFP inoculated. To accomplish this, we examined the H&E stained paraffin sections of bladder tumors and compared them with the *in vivo* GFP image and the image of the transversally sliced gross bladders. Once confirmed, we proceeded to measure the bladders and tumors. Tumor size measurements are represented by tumor area and tumor area percent and were calculated by histological analysis and GFP expression. Tumor area is defined a the area of positive GFP emitting regions of green

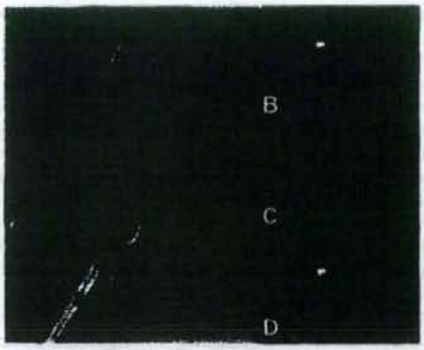

Figure 1. The anatomical view of the nude mouse during the urinary catheterization procedure (A). *In vivo* digital images were obtained by first making a transverse incision across the lower abdomen to expose the bladder. The exposed bladder was filled with PBS an image was acquired using a tungsten light source (B). The bladder was then exposed to a 470-nm wavelength blue light and an image was captured through a 530-nm wavelength emission filter (C). The two images are merged together for the purpose of demonstrating the anatomical location of GFP-labeled tumor cells within the bladder *in vivo* (D).

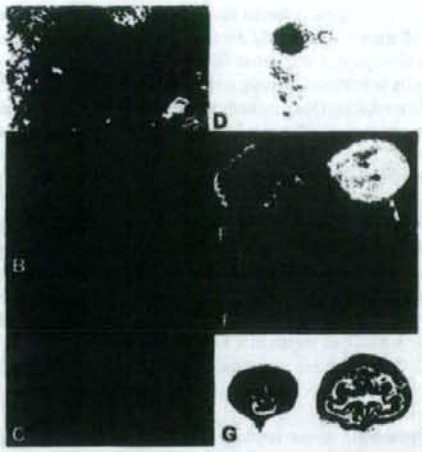

Figure 2. Bladder images were captured under tungsten light (A) and fluorescent light (B) *in vivo*. The raw unmanipulated image was then adjusted and corrected to remove non-specific fluorescence (C). Non-specific fluorescence was subtracted from the background by adjusting contrast and brightness and selecting the appropriate maximum and minimum light and dark set-levels for each individual image. The corrected image was converted to a 16-bit inverted grayscale image, and a mask using color-coded contour lines corresponding to light intensity (corresponding to GFP expression) was applied to identify the tumor (D). Tumor tissue (arrows) was confirmed with the gross bladder (E-F) and the corresponding H&E stained section (G).

fluorescent light in the images captured *in vivo* or regions of tumor bounded by the ROI in selected histological slides. All area measurements are represented by mm². To avoid possible differences that may have occurred by having bladders expanded to different diameters, we calculated the tumor area percent. Tumor area percent represents the percent of bladder area comprised of tumor. Regression analysis determined the R^2 values for tumor area and tumor area percent to be 0.281 and 0.692, respectively (Fig. 4). Doxorubicin efficacy against tumor growth resulted in a 9- and 12-fold decrease of tumor area when measured by histological analysis and GFP expression, respectively (Fig. 5A). Similarly, a 5- and 9.25-fold difference in tumor growth was noted when

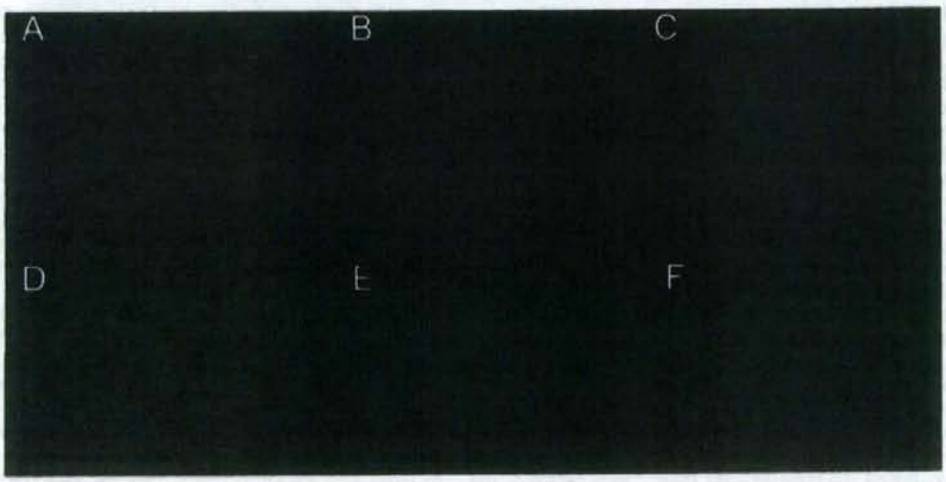

Figure 3. Representative images of bladders taken under a fluorescent light source demonstrate the presence of KU-7/GFP cells by the emission of green fluorescent light. No tumor is present in (A) and as small microscopic lesion is visible (B). Tumors may appear as multiple tumor clusters of varying sizes (C-E) or as a large mass (F).

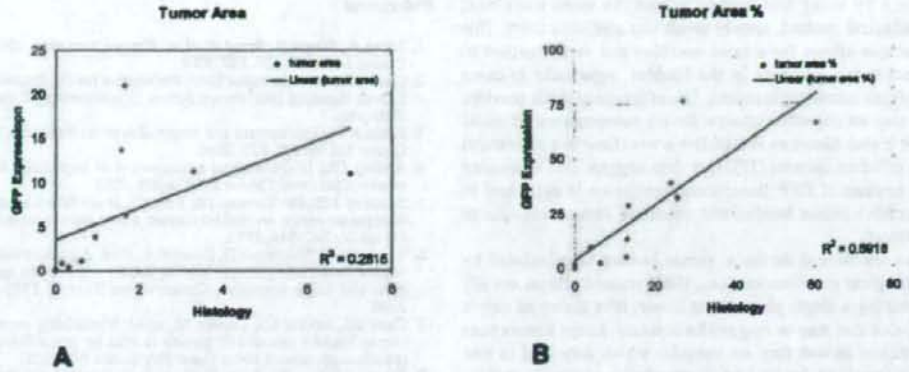

Figure 4. Correlation of tumor area (A) and tumor area percent (B) for all mice bearing KU-7/GFP orthotopic bladder tumors (n=10). GFP expression was plotted against histology examination.

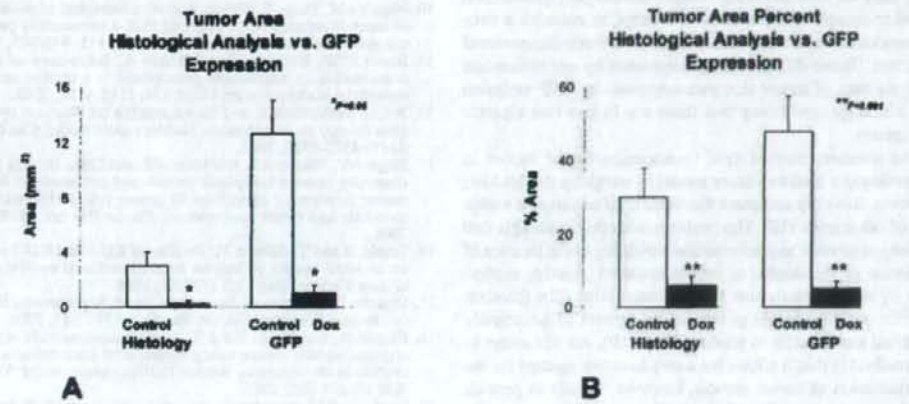

Figure 5. Comparison of tumor response to doxorubicin graphed as tumor area (A) and tumor area percent (B) by GFP expression and histological analysis. *, **P-values versus control, Student's t-test analysis.

measuring tumor response as a percent of the total bladder area as measured by histological analysis and GFP expression, respectively (Fig. 5B).

Although correlation analysis does not demonstrate a strong correlation between tumor sizes measured by GFP and histological analysis, reproducibility and sensitivity were greater by using GFP analysis alone. Similar results were obtained by repeating similar experiments at varying time points (data not shown).

Discussion

The orthotopic bladder cancer model has proven to be one of the most effective models to study tumor biology, particularly in studies involving intravesical therapy. This is due to the fact that tumors are directly exposed to the chemotherapeutic agents in their natural environment (15). Unlike ectopic xenograft models that grow easily visible subcutaneous tumors, bladder orthotopic models grow tumors internally that cannot be visualized grossly *in vivo* and thus renders a challenge to confirm tumor incidence, growth and response. Traditional methods to determine tumor burden in the orthotopic bladder cancer model consist of weighing the bladder and histological analysis (16). However, sensitivity and objectivity in measuring tumor burden is limited due to variability of bladder and tumor size, especially in the case of microscopic disease. Use of GFP-labeled bladder cancer cells in the orthotopic bladder cancer model provides an added means to qualitatively identify such tumors *in vivo*, however, precise and objective quantitative methods have yet to be developed.

The focus of this experiment is to establish a method to measure tumor size in an objective and efficient manner. We compared sensitivity, objectivity and efficiency in measuring tumor response after chemotherapeutic treatment with doxorubicin against the more traditional histological evaluation method. Our results clearly elucidate some of the benefits

gained by using this method versus the more traditional histological method, namely sensitivity and objectivity. This technique allows for a more sensitive and faster method to detect tumor presence in the bladder, especially in cases involving microscopic lesions. Use of image analysis provides not only an objective solution for the interpretation of visual data; it also allows us to establish a workflow in a convenient and efficient manner (17). Our data suggest that measuring the amount of GFP fluorescence emission is sufficient to determine tumor burden and calculate tumor response to treatment.

In traditional methods, tumor burden is calculated by histological examination (i.e., H&E stained slides) usually examining a single plane of the tumor, thus giving us only a snapshot that may or may not be accurate. Large tumors pose a problem in that they are irregular which may lead to bias when searching for the best representative section to analyze and quantify. Furthermore, small tumors present a different problem in that they may be too small to accurately capture in a thin section and may therefore lead to inaccuracies as they may be missed during routine histological procedures. Another complication is that we attempt to examine a two-dimensional object and interpret it as a three-dimensional structure. These differences are supported by our correlation analysis data of tumor size measurements by GFP emission and histology confirming that these are in fact two separate parameters.

An alternate method used to determine tumor burden in the orthotopic bladder cancer model is weighing the bladder; however, this only compares the bladder of one mouse versus that of other mice (18). The problem with this method is that it does not provide any information pertaining to the location of the lesion or the number of lesions involved. Another method used by some investigators is to measure urine PSA (prostate specific antigen) levels generated by tumors of genetically modified cancer cells to produce PSA (19). An advantage to this method is that it allows for a non-invasive method for the determination of tumor growth, however, it fails to provide any insight into the morphological dynamics including the number of tumors present or tumor distribution and location in the bladder. Use of bioluminescent particles, such as firefly luciferase, coupled with image analysis allow for accurate *in vivo* measurements of labeled tumors (20,21). The drawback to this method is the investment involved as it requires specialized dedicated imaging equipment for imaging small animals.

Our results demonstrate that using computer assisted image analysis to measure GFP expression, as a parameter for the determination tumor response to therapy in the mouse orthotopic bladder model, serves as a powerful and objective tool proving to be more sensitive than histology. Additionally, using this method allows the investigator to conduct more labor-effective and cost-effective experiments with minimal investment. Furthermore, this methodology is not limited to the orthotopic bladder cancer model as it can be applied to other tumor models requiring precise objective quantitative analysis of tumor size.

References

1. Jemal A, Siegel R, Ward E, *et al*: Cancer Statistics, 2006. CA Cancer J Clin 56: 106-130, 2006.
2. Cancer Statistics in Japan 2005; Foundation for the Promotion of Cancer Research (http://www.fpcr.or.jp/publication/pdf/statistics 2005.pdf).
3. Kakizoe T: Development and progression of urothelial carcinoma. Cancer Sci 97: 821-828, 2006.
4. Amling CL: Diagnosis and management of superficial bladder cancer. Curr Probl Cancer 25: 224-278, 2001.
5. Soloway MS, De Kernion JB, Rose D, *et al*: Effect of chemotherapeutic agents on bladder cancer: a new animal model. Surg Forum 24: 542-544, 1973.
6. Watanabe T, Shinohara N, Sazawa A, *et al*: An improved intravesical model using human bladder cancer cell lines to optimize gene and other therapies. Cancer Gene Ther 7: 1575-1580, 2000.
7. Zhou JH, Rosser CJ, Tanaka M, *et al*: Visualizing superficial human bladder cancer cell growth *in vivo* by green fluorescent protein expression. Cancer Gene Ther 8: 681-686, 2002.
8. Tanaka M, Gee JR, De la Cerda J, *et al*: Noninvasive detection of bladder cancer in an orthotopic murine model with green fluorescence protein cytology. J Urol 3: 975-978, 2003.
9. Caceres G, Zhu XY, Jiao JA, *et al*: Imaging of luciferase and GFP-transfected human tumours in nude mice. Luminescence 24: 218-223, 2003.
10. Nogawa M, Yuasa T, Kimura S, *et al*: Intravesical administration of small interfering RNA targeting PLK-1 successfully prevents the growth of bladder cancer. J Clin Invest 115: 978-985, 2005.
11. Brocks CP, Buttner H and Bohle A: Inhibition of tumor implantation by intravesical gemcitabine in a murine model of superficial bladder cancer. J Urol 174: 1115-1118, 2005.
12. Wu Q, Mahendran R and Esuvaranathan K: Nonviral cytokine gene therapy on an orthotopic bladder cancer model. Clin Cancer Res 9: 4522-4528, 2003.
13. Singh AV, Franke AA, Blackburn GL and Zhou JR: Soy phytochemicals prevent orthotopic growth and metastasis of bladder cancer in mice by alterations of cancer cell proliferation and apoptosis and tumor angiogenesis. Cancer Res 66: 1851-1858, 2006.
14. Tazaki H and Tachibana M: Studies on KU-1 and KU-7 cells as an *in vitro* model of human transitional cell carcinoma of urinary bladder. Hum Cell 1: 78-83, 1988.
15. Oliveira PA, Colaco A, De la Cruz, *et al*: Experimental bladder carcinogenesis-rodent models. Exp Oncol 28: 2-11, 2006.
16. Hegele A, Dalpke A, Heeg K, *et al*: Immunostimulatory CpG oligonucleotides reduce tumor burden after intravesical administration in an orthotopic murine bladder cancer model. Tumour Biol 26: 274-280, 2005.
17. Hoffman RM: Imaging tumor angiogenesis with fluorescent proteins. APMIS 112: 441-449, 2004.
18. Gunther JH, Prambach M, Deinert I, *et al*: Effects of acetylic salicylic acid and pentoxifylline on the efficacy of intravesical BCG therapy in orthotopic murine bladder cancer (MB49). J Urol 161: 1702-1706, 1999.
19. Wu Q, Esuvaranathan K and Mahendran R: Monitoring the response of orthotopic bladder tumors to granulocyte macrophage colony-stimulating factor therapy using the prostate-specific antigen gene as a reporter. Clin Cancer Res 10: 6977-6984, 2004.
20. Ponomarev V, Doubrovin M, Serganova I, *et al*: A novel triple-modality reporter gene for whole-body fluorescent, bioluminescent, and nuclear noninvasive imaging. Eur J Nucl Med Mol Imaging 31: 740-751, 2004.
21. Yanagihara K, Takigahira M, Takeshita F, *et al*: A photon counting technique for quantitatively evaluating progression of peritoneal tumor dissemination. Cancer Res 66: 7532-7539, 2006.

Identification of Annexin 1 as a Novel Autoantigen in Acute Exacerbation of Idiopathic Pulmonary Fibrosis[1]

Katsushi Kurosu,[2]* Yuichi Takiguchi,* Osamu Okada,* Norio Yumoto,* Seiichiro Sakao,* Yuji Tada,* Yasunori Kasahara,* Nobuhiro Tanabe,* Koichiro Tatsumi,* Michael Weiden,† William N. Rom,† and Takayuki Kuriyama*

Consistent with the hypothesis that pulmonary epithelial apoptosis is the key to the acute exacerbation of idiopathic pulmonary fibrosis (IPF), we conducted serological identification of Ags by recombinant expression cloning (SEREX) analysis using type II alveolar cell carcinoma (A549) cell lines to identify disease-related Abs. In a survey of Abs to the recombinant autoantigens identified by SEREX analysis, five Abs were identified as novel candidates for the acute exacerbation of IPF. Abs to annexin 1 were detected in 47 and 53% of the sera and bronchoalveolar lavage materials from patients with acute exacerbation of IPF. Some identical TCR Vβ genes were identified in sequential materials obtained at 1–3 mo in all 10 acute exacerbation IPF cases, suggesting that some infiltrating CD4-positive T cells sharing limited epitopes expand by Ag-driven stimulation during disease extension. The CDR3 region of these identical TCR Vβ genes showed high homology with the N-terminal portion of annexin 1, including in the HLA-DR ligand epitopes predicted by TEPITOPE analysis. By Western blotting analysis and observation of the CD4-positive T cell responses in bronchoalveolar lavage samples, the N-terminal portion of annexin 1 was cleaved and found to induce marked proliferative responses of CD4-positive T cells in three patients. Our study demonstrates that annexin 1 is an autoantigen that raises both Ab production and T cell response in patients with acute exacerbation of IPF, and that the N-terminal portion of annexin 1 plays some role in the pathogenesis of acute exacerbation in IPF patients. ***The Journal of Immunology*****, 2008, 181: 756–767.**

Idiopathic pulmonary fibrosis (IPF)[3] is a chronic lung disease of unknown cause that is limited to the lungs and is associated with a histological pattern of usual interstitial pneumonia on lung biopsy. Basal and peripheral reticular opacities associated with traction bronchiectasis and honeycombing are typical high-resolution computed tomography signs of IPF, and these findings, combined with the clinical profile, are sufficient to establish a confident diagnosis of IPF (1). The natural history is invariably one of gradual and progressive deterioration resulting in scarring, pulmonary failure, and death, with the median length of survival from the time of diagnosis ranging from 2.5 to 3.5 years. The pathogenesis of the disease is unknown, but it may involve an immunological reaction to unidentified Ags in the lung related to tissue damage. Although chronic in nature, it has been reported that an important complication is an accelerated phase of the disease, leading to death in a period of weeks to a few months, and that open-lung biopsy performed after exacerbation confirms an acute diffuse alveolar damage pattern together with chronic interstitial pneumonia of the usual interstitial pneumonia type (2). It remains uncertain what causes such accelerated clinical deterioration (3).

Immunohistochemical data demonstrate the presence of circulating IgG Abs to endogenous autoantigens on pulmonary epithelial cells in IPF patients (4, 5). Although antinuclear Abs, anti-DNA topoisomerase II Abs, and Abs to cytokeratin 8 (6) have been demonstrated in IPF patients, there are no reports of Abs related to the acute exacerbation of IPF. Serological identification of Ags by recombinant expression cloning (SEREX) is a well-established and powerful technique that has been applied to Ag-specific IgG responses in a variety of tumor systems and some autoimmune diseases (7, 8). The suitability of the SEREX approach to define autoantigens associated with autoimmune diseases such as systemic lupus erythematosis (SLE) and systemic sclerosis has been shown. These studies indicate that a thorough evaluation of autoantigen reactivity patterns of sera from patients suffering from various autoimmune diseases is critical for estimating the diagnostic value and potential pathogenic role of these Ags (9–11). Apoptotic alveolar epithelial cells are detected primarily in areas of IPF that appear histologically normal without established fibrosis (12) and are adjacent to underlying foci of myofibroblasts (13). Recent studies have implicated apoptosis of alveolar epithelial cells as a potential initiating mechanism in the development of pulmonary injury and fibrosis. Data obtained using animal models have provided some insights into whether excessive apoptosis of alveolar epithelial cells may be the primary event leading to lung fibrosis. It has been demonstrated that repeated inhalations of agonistic anti-Fas Abs induce apoptosis of alveolar epithelial cells, leading to pulmonary fibrosis in mice (14). The targeted transgenic

*Department of Respirology (B2), Graduate School of Medicine, Chiba University, Chiba, Japan; and †Division of Pulmonary and Critical Care Medicine, Department of Medicine, School of Medicine, New York University, New York, NY 10016

Received for publication June 12, 2007. Accepted for publication April 27, 2008.

The costs of publication of this article were defrayed in part by the payment of page charges. This article must therefore be hereby marked *advertisement* in accordance with 18 U.S.C. Section 1734 solely to indicate this fact.

[1] This work was supported in part by a grant for scientific research from the Japanese Ministry of Education (15590798).

[2] Address correspondence and reprint requests to Dr. Katsushi Kurosu, Department of Respirology (B2), Graduate School of Medicine, Chiba University, 1-8-1 Inohana, Chuo-ku, Chiba 260-8670, Japan. E-mail address: kurosu@faculty.chiba-u.jp

[3] Abbreviations used in this paper: IPF, idiopathic pulmonary fibrosis; SEREX, serological analysis of the cDNA expression library; SLE, systemic lupus erythematosis; RA, rheumatoid arthritis; BAL, bronchoalveolar lavage; TGF, transforming growth factor; VATS, video-associated thoracic surgery; IP-CVD, interstitial pneumonia related to collagen vascular disease; PM/DM, polymyositis/dermatomyositis; Ssc, scleroderma; HP, hypersensitivity pneumonitis; ER, endoplasmic reticulum.

Table I. *Molecular details of the cases of acute exacerbation of IPF*

Case No.	Age/Sex	Specimens	BAL Profile[b] Cellularity (10^6/ml)	% Mac	% Lym	% Neu	% Eos	CD4/CD8	Predominant TCR-Vβ Usages	MHC Allele	Outcome
1	74/F	BAL	2.1	56	15	28	5	1.78	2, 3,[a] 5,[a] 7, 9[a]	DRB1*0403 and *0410	Deceased
		BAL and autopsy (2 mo later)	2.4	44	18	36	2	2.83	4, 3,[a] 5,[a] 8, 9[a]		
2	65/M	BAL	1.6	67	15	18	0	2.55	2, 6,[a] 9	DRB1*0802 and *1401	Deceased
		BAL and autopsy (3 mo later)	3.4	53	10	34	3	1.96	6,[a] 10, 16		
3	69/F	BAL	3.8	51	15	32	2	2.84	4, 9,[a] 14,[a] 15[a]	DRB1*1307 and *1502	Deceased
		BAL and autopsy (1 mo later)	3.3	28	18	46	8	3.56	9,[a] 14,[a] 15,[a] 21		
4	62/M	BAL	2.6	70	16	12	2	1.35	7,[a] 9,[a] 14,[a] 24	DRB1*0101 and *0410	Deceased
		BAL and autopsy (2 mo later)	2.5	47	24	21	8	1.54	7,[a] 9,[a] 14[a]		
5	71/M	BAL	1.4	74	12	8	6	0.54	4,[a] 5,[a] 21	DRB1*0101 and *1501	Deceased
		BAL and autopsy (3 mo later)	2.2	60	6	28	6	1.02	4,[a] 5,[a] 16		
6	58/M	VATS							1, 2,[a] 12,[a] 14	DRB1*0401 and *1602	Surviving
		BAL (2 mo later)	1.4	65	17	14	4	1.68	2,[a] 12,[a] 16, 20		
7	59/F	VATS							3, 14, 19[a]	DRB1*0901 and *1001	Surviving
		BAL (2 mo later)	2.3	62	6	28	4	0.48	9, 10, 19[a]		
8	62/F	BAL	3.2	54	2	42	2	2.42	1, 7,[a] 10,[a] 20[a]	DRB1*0403 and *1502	Deceased
		BAL (1 mo later)	3.6	38	8	48	6	3.86	2, 7,[a] 10,[a] 20[a]		
9	62/M	BAL	2.5	59	13	18	10	1.24	3,[a] 8, 12, 18[a]	DRB1*0405 and *1101	Surviving
		BAL (2 mo later)	3.8	50	14	28	8	1.89	3,[a] 18,[a] 22		
10	66/M	VATS	1.7	63	12	23	2	1.54	2, 4,[a] 10, 18	DRB1*0406 and *1405	Surviving
		BAL (2 mo later)	3.2	60	8	26	6	1.98	4,[a] 11, 14		
11	68/M	BAL	3.4	65	6	25	4	0.68	3, 5, 8, 10	DRB1*1201 and *1302	Deceased
12	65/M	BAL	2.8	64	10	23	3	3.88	2, 10, 14	DRB1*0405 and *0803	Surviving
13	72/F	BAL	2.8	64	8	24	4	0.55	6, 12	DRB1*1403 and *0901	Deceased
14	70/M	BAL	3.4	48	12	32	8	2.89	1, 3, 10, 18	DRB1*1202 and *1501	Surviving
15	68/F	BAL	4.1	88	4	8	0	0.35	2, 5, 9	DRB1*0405 and *0803	Surviving

[a] Identical oligoclonal expansions were detected in both the first BAL/VATS and subsequent BAL materials by RT-PCR and sequencing analysis.
[b] Mac indicates macrophages; Lym, lymphocytes; Neu, neutrophils; Eos, eosinophils.

overexpression of bioactive TGF-β1 in the murine lung produces a transient wave of epithelial apoptosis followed by mononuclear rich inflammation, tissue fibrosis, myofibroblast hyperplasia, and honeycombing (15). The induction of lung fibrosis by intratracheal instillation of bleomycin was reported to be associated with the up-regulation of Fas on the epithelium and with the concomitant induction of epithelial apoptosis as a prelude to fibrogenesis (16). Consistent with the hypothesis that epithelial pathology, particularly pulmonary epithelium apoptosis, is the key to IPF pathogenesis, and that it might have some role in the acute exacerbation of IPF, we conducted SEREX analysis using a cDNA phage library of type II alveolar cell carcinoma (A549) cell lines to identify specific Abs present in sera from acute exacerbation of IPF patients compared with stable IPF cases.

Examination of affected pulmonary tissues from IPF patients reveals inflammatory infiltrates composed principally of T lymphocytes and macrophages, with variable numbers of neutrophils, eosinophils, and mast cells and B lymphocyte aggregates. The oligoclonality of TCR gene usage has been demonstrated in a variety of diseases, including IPF (17), sarcoidosis (18), rheumatoid arthritis (RA) (19), and a variety of other immune-mediated diseases. Our experiments also include an analysis of the TCR Vβ repertoire of CD4-positive T cells in bronchoalveolar lavage (BAL) fluid derived from acute exacerbation of IPF patients. Some identical TCR Vβ genes were identified first in BAL or video-associated thoracic surgery (VATS) material and sequential second BAL materials obtained during 1–3 mo in all 10 cases of acute exacerbation of IPF (cases 1–10) analyzed, suggesting that some infiltrating CD4-positive T cells share limited epitopes on some Ags and continue to expand oligoclonally by Ag-driven stimulation in the alveolar spaces during disease extension. The overlap of immunodominant T and B cell epitopes has been reported in diazepam-binding inhibitor-related protein 1 for aplastic anemia (20), pyruvate dehydrogenase complex for primary biliary cirrhosis (21), and myelin basic protein for multiple sclerosis (22), suggesting that overlap of T and B cell reaction is a common theme for autoimmune reaction in several diseases. To examine our hypothesis that Abs detected in our SEREX analysis might recognize Ags that elicit T cell response in patients with acute exacerbation of IPF, we used the MHC class II epitope prediction program (TEPITOPE) analysis to investigate promiscuous HLA-DR ligands of autoantigens related to acute exacerbation of IPF as defined by the SEREX approach. Our study demonstrates that annexin I is an autoantigen that raises both Ab production and T cell response in patients with acute exacerbation of IPF, and that the N-terminal portion of annexin I plays some important role in the pathogenesis of the acute exacerbation of IPF patients.

Materials and Methods

Patients

The diagnosis of IPF was based on standard criteria that included clinical findings, pulmonary function tests, and chest radiographic and high-resolution computed tomography findings (23). An acute exacerbation in patients with IPF was defined as follows: for the accelerated phase of IPF, exacerbation of dyspnea within 1 mo, new diffuse pulmonary opacities on chest radiography, a decrease in PaO_2 of 10 mmHg, and an absence of infection or heart failure. We defined stable IPF as IPF without acute exacerbation (24). BAL fluids and sera were collected from 45 patients with IPF (15 acute exacerbation patients, 30 stable patients), 90 patients with interstitial pneumonia related to collagen vascular disease (IP-CVD) (20 polymyositis/dermatomyositis (PM/DM) patients, 20 Sjögren syndrome patients, 20 scleroderma (Ssc) patients, 20 RA patients, 10 SLE patients), 30 patients with pulmonary sarcoidosis, 10 patients with chronic eosinophilic pneumonia, 10 patients with hypersensitivity pneumonitis (HP), and 40 normal volunteers; all samples were stored at −80 °C until use. Autopsies were conducted on five patients with acute exacerbation of IPF (cases 1–5). At the time of autopsy, BAL fluids were also collected. In another five patients (cases 6–10), a second BAL analysis was performed 1–2 mo after VATS or the first BAL procedure (Table I). This study was approved by the Ethical Committee of Chiba University.

Construction of a cDNA library and immunoscreening

mRNA was extracted by a Quick Prep mRNA purification kit (Amersham Biosciences) from A549 cells as recommended by the manufacturer. A total of 5 mg mRNA was used for the construction of the ZAP expression library (ZAP-cDNA synthesis kit, ZAP-cDNA Gigapack III Gold cloning

Table II. *Autoantigen genes identified by SEREX in IPF patients*

Designation	Cases: Acute Exacerbation of IPF (n = 15, cases 1–15)	Cases: Stable IPF (n = 30, cases 16–45)	Homology to Published Sequences in the GenBank Database (Accession No.)	Amino Acid No.: Full Length	Amino Acid No.: Ags Identified by SEREX	Amino Acid No.: Recombinant Proteins: Length[b]	Amino Acid No.: Recombinant Proteins: Amino Acid Position
AG1	1, 2, 3, 5, 8, 12, 14[a]	24, 32	Annexin 1 (NM_000700)	328–335	347	335	8–342
AG2	2, 5, 9, 12, 15[a]	25, 30, 33	Bax inhibitor 1 (BC_036203)	187–230	238	232	7–238
AG3	7, 8, 10, 13	28, 35	Cytochrome c oxidase subunit 5a (BC_024240)	151	151	151	1–151
AG4	4, 10, 14	26	Heme oxygenase 1 (HMOX1) (AY_460337)	287	289	263	25–287
AG5	1, 5, 11	30	Phosphoglycerate kinase 1 (S 75476)	310	418	408	3–410
AG6	3, 13	21, 37, 42	Annexin 4 (M_82809)	255–322	322	319	1–319
AG7	11	22, 38	Macrophage migration inhibitory factor (BC_022414)	110–114	116	115	2–116
AG8	12	24, 36	Aldehyde dehydrogenase 1 A1 (M_31994)	242–308	502	432	29–460
AG9	9	22, 40	Cytochrome c1 (BC_015616)	263–324	326	276	46–321
AG10		28	Annexin 2 (BC_001388)	329	340	331	2–332
AG11		34	Cytochrome c reductase core protein 1 (L_16842)	386	490	424	49–472
AG12		20, 26	Cytokeratin 8 (BC_073760)	400–412	484	450	5–454

[a] In acute exacerbation of IPF cases, the most frequently isolated genes were annexin 1 and Bax inhibitor 1, comprising 7 of 15 cases (47%) and 5 of 15 cases (33%), respectively.

[b] The recombinant protein of cytochrome c oxidase subunit 5a represents full-length products, whereas the other 11 recombinant autoantigens represent almost full-length products.

kit; Stratagene). The titer of each of these cDNA expression libraries was on average 2.0×10^6 PFU/ml. Immunological screening was performed essentially as described (25). In the screening steps, we isolated plaques that reacted strongly with sera from IPF patients but remained undetectable in sera from normal volunteers. Positive phagemids were submitted to in vivo excision of the pBluescript plasmid (Stratagene), which was then sequenced.

Expression of recombinant autoantigens in Escherichia coli *cells and Ab assay*

All 12 autoantigens identified by our SEREX analysis were expressed in *E. coli* (M15 cells) using 6Xhistidine tag-containing vector pQE30 (Qiagen). Various cDNA amplification primers were designed to encompass almost the entire coding sequences of these genes, corresponding to the amino acid positions shown in Table II. The induction of recombinant protein synthesis and subsequent purification on Ni-NTA spin columns (Qiagen) were conducted as instructed by the manufacturer. Using Ni-NTA HisSorb plates (Qiagen) coated with these 6Xhistidine tag proteins, autoantibody activities in the BAL samples and sera were measured by ELISA as described previously (26). A positive reaction was defined as one with an OD value that differed from that of sera from normal donors (n = 40) by 3 SDs.

PCR amplification and sequencing of TCR Vβ genes of CD4-positive lymphocytes from BAL or VATS samples of IPF patients

BAL was conducted using a standard technique as previously described (27). Briefly, four 50-ml boluses of 37°C prewarmed sterile 0.9% saline were instilled by inserting the bronchoscope into a segmental bronchus of the right middle lobe, lingula, or lower lobes and were gently aspirated via a hand-held syringe. Total cell count was determined by using a hemocytometer. A differential cell count was taken on Giemsa-stained cytocentrifuged preparations. Following cell count, part of the cell mass was subjected to flow cytometric analysis. Some cells (2×10^5) were stained with MoAb against Leu4 (anti-CD3), Leu3a (anti-CD4), and Leu2a (anti-CD8) (BD Biosciences). CD4-positive lymphocytes were isolated from BAL fluid and peripheral blood lymphocytes using anti-CD4 mAb-coated Dynabeads (Dynal Biotech) according to the method described by the manufacture. Total RNA from CD4-positive cells isolated from BAL fluid were prepared with Isogen (Nippon Gene). PCR and cDNA synthesis and the oligonucleotide primers used for amplification of the TCR Vβ genes were described before (28). PCR amplification of the TCR Vβ genes of the cDNA was performed in multiple tubes, with each tube containing one of the TCR Vβ subfamily primers and Cβ primer. For Southern blot analysis, the PCR products (20 μl) were subjected to 2% agarose gel electrophoresis and then transferred to a nylon membrane. The membranes were hybridized with oligonucleotide Cβ probe labeled with a fluorescein-dUTP labeling kit (Amersham Biosciences) at the 3′ends, and visualized using a CDP-Star detection module followed by autoradiography with Hyperfilm-MP (both from Amersham Biosciences). All PCR products demonstrating amplification of the same TCR Vβ repertoires in both the first BAL fluid or VATS materials and sequential BAL samples were ligated to plasmids using the TA cloning kit (Invitrogen), transformed into competent *E. coli* cells, and grown under appropriate conditions. After selection of TCR Vβ-positive colonies, plasmid DNA was purified. Inserts in the PCR vector were sequenced by the Dye Primer method using a *Taq* Dye Primer Cycle Sequencing Core kit (Applied Biosystems). All clones were sequenced from both directions using M13 forward and reverse primers. The TCR Vβ sequences were analyzed using the international ImMunoGeneTics (IMGT) database (http://imgt.cines.fr) (29).

Molecular typing of HLA-DR molecules and the TEPITOPE analysis

Typing of HLA-DR alleles was performed using a Dynal RELI SSO HLA-DRB typing kit (Dynal Biotech). TEPITOPE software (http://www.tepitope.com) was used to predict potential HLA-DR-binding peptides within autoantigens identified by SEREX analysis with a prediction threshold of 3%. These HLA-DR-binding peptides were compared with the CDR3 regions of identical TCR Vβ genes of CD4-positive lymphocytes from first BAL or VATS and sequential BAL samples from acute exacerbated IPF patients.

Western blot analysis of annexin 1 in BAL samples from IPF patients and non-IPF BAL samples and CD4-positive T cell responses in BAL fluid to N-terminal annexin 1 peptides

BAL fluids were concentrated 10-fold by centrifugation using Amicon Centricon 10 filters (Millipore). BAL samples equivalent to 50 μg protein were subjected to SDS-PAGE under denaturing conditions. In addition to BAL samples from 15 acute exacerbation of IPF cases, BAL materials from 30 stable IPF patients and non-IPF patients (90 patients with collagen vascular disease, 30 patients with pulmonary sarcoidosis, 10 patients with eosinophilic pneumonia, 10 patients with HP, and 40 normal volunteers) were analyzed. After electrophoresis, the proteins were electrotransferred to a nylon membrane and probed with polyclonal annexin 1 Ab (sc-11387, Santa Cruz Biotechnology) against amino acids (position 235–299) of human annexin 1, and visualized with HRP-conjugated anti-rabbit IgG Ab and a chemiluminescent substrate system (Amersham Biosciences).

We analyzed whether N-terminal peptides of annexin 1 elicit CD4-positive T cell responses in BAL samples from patients with acute exacerbation of IPF (cases 1, 3, 5, 6, 7, and 9). Three patients (cases 1, 3, and 5)

Table III. *Characteristics of BAL fluid of the study population*

Ag (Designation)	IPF		IP-CVD	Pulmonary Sarcoidosis	Eosinophilic Pneumonia	HP	Normal Volunteers
	Acute Exacerbation	Stable					
Subjects (n)	15	30	90	30	10	10	40
Cellularity (10^6/ml)	3.0	1.8	2.6	2.8	3.2	2.9	0.8
Macrophages (%)	58 (28–74)	96 (86–98)	84 (65–96)	75 (64–88)	63 (56–82)	66 (62–76)	96 (90–99)
Lymphocytes (%)	12 (2–24)	2 (0–10)	14 (4–32)	24 (12–34)	8 (0–18)	32 (24–36)	4 (0–9)
Neutrophils (%)	26 (8–48)	0 (0–6)	1 (0–8)	1 (0–4)	3 (0–8)	1 (0–4)	0 (0–3)
Eosinophils (%)	4 (0–10)	0 (0–4)	1 (0–8)	0 (0–4)	26 (18–36)	1 (0–4)	0 (0–4)

displayed high titers of anti-annexin I Abs, and the CDR3 regions of identical TCR Vβ genes (clones 1-1, 3-1, and 5-1) from the first BAL and second sequential biopsies from those cases showed high homology with the same portion (residues 18–26) of annexin I included in the epitopes of the autoantigens predicted by TEPITOPE analysis. In contrast, the other patients (cases 6, 7, and 9) were negative for anti-annexin I Abs. CD4-positive T cells were separated from BAL cells using anti-CD4 mAb-coated Dynabeads (Dynal Biotech). For purification of alveolar macrophages, BAL cells were allowed to adhere to plastic plates for 3 h. Cells were recovered by gentle scraping with a rubber policeman. The alveolar macrophages thus obtained were 95% pure by morphology and nonspecific esterase staining. A total of 5×10^4 CD4-positive T cells were cultured in 96-well U-bottom plates (Iwaki Glass) with the same number of alveolar macrophages for 6 days at 37°C with medium only, N-terminal annexin I-positive peptide (20 μg/ml, position 18–26: QEYVQTVKS), or a negative peptide (20 μg/ml, position 201–209: DARALYEAG) of annexin I predicted to display no binding to the HLA molecule. After triplicate cultures were maintained for 6 days, the BrdU assay procedure was conducted using a Frontier BrdU cell proliferation assay cell proliferation kit (Funakoshi) according to the protocol of the manufacturer. The reaction was quantified by measuring the OD at a wavelength of 450 nm.

In vitro assay of lymph node cells for annexin I Ab production

An in vitro assay to analyze annexin I peptide-induced anti-annexin I Ab synthesis of lymph node cells from patients with acute exacerbation of IPF (cases 1, 3, and 4) was conducted. Two patients (cases 1 and 3) displayed high titers of anti-annexin I Abs, and the other patient (case 4) was negative for anti-annexin I Ab. Hilar lymph nodes dissected at the time of autopsy were forced through sterile mesh screens, and the cells were repeatedly washed and resuspended in complete medium. B cells and $CD4^+$ and $CD8^+$ T cell subsets were negatively selected by the MACS magnet-activated cell separation system (Miltenyi Biotec) as instructed by the manufacturer. Either $CD4^+$ or $CD8^+$ subsets of T cells (10^5/well) with the same number of purified B cells as well as B cells alone were cocultured in 24-well tissue culture plates with N-terminal annexin I-positive peptide (20 μg/ml, position 18–26: QEYVQTVKS) or -negative peptide (20 μg/ml, position 201–209: DARALYEAG) of annexin I in the presence of pokeweed mitogen (1 μg/ml) for 10 days. Anti-annexin I Ab levels in undiluted culture supernatants were measured by ELISA using Ni-NTA HisSorb plates coated with 6Xhistidine tag annexin I proteins as described above. The reaction was quantified by measuring the OD at a wavelength of 450 nm. All cultures were prepared in duplicate, and anti-annexin I Ab results represent the means of duplicate values.

Western blot analysis of full-length and elastase-cleaved annexin I probed with BAL and sera from IPF patients and non-IPF patients

The cDNA amplification primers were designed to encompass the entire coding sequence of annexin I. The primer sequences for annexin I (sense, ATGGCAATGGTATCAGAA and anti-sense, GTTTCCTCCACAAA GAGC) were used for amplification of annexin I cDNA from A549 cDNA library by PCR (30 cycles). After nucleotide sequencing of PCR products was determined by the Dye Primer method using a *Taq* Dye Primer Cycle

Table IV. *Frequency (percentage) of ELISA reactivity with recombinant autoantigens*

Ag (Designation)	IPF		IP-CVD (n = 90)					Pulmonary Sarcoidosis	Eosinophilic Pneumonia	HP	Normal Volunteers
	Acute Exacerbation (n = 15)	Stable (n = 30)	PM/DM (n = 20)	Sjögren (n = 20)	Ssc (n = 20)	RA (n = 20)	SLE (n = 10)	(n = 30)	(n = 10)	(n = 10)	(n = 40)
Serum reactivity											
AG1	47	7	0	0	0	10	10	0	0	0	0
AG2	33	10	0	0	0	0	0	0	0	0	0
AG3	27	7	0	0	0	0	5	0	0	0	0
AG4	20	3	0	0	0	5	0	0	0	0	0
AG5	20	3	0	0	0	10	0	0	0	0	0
AG6	13	10	0	0	0	0	0	0	0	0	0
AG7	7	7	0	0	0	0	0	0	0	0	0
AG8	7	7	0	5	0	0	0	0	0	0	0
AG9	7	7	0	0	0	0	0	0	0	0	0
AG10	0	3	0	0	0	5	0	0	0	0	0
AG11	0	3	0	0	0	0	0	0	0	0	0
AG12	0	7	0	0	0	0	0	0	0	0	0
BAL fluid reactivity											
AG1	53	10	0	0	0	0	0	0	0	0	0
AG2	33	7	0	0	0	0	5	0	0	0	0
AG3	33	7	0	5	0	0	0	0	0	0	0
AG4	33	3	0	0	0	0	0	0	0	0	0
AG5	27	3	0	0	0	0	0	0	0	0	0
AG6	13	13	0	0	0	0	0	0	0	0	0
AG7	7	10	0	0	0	0	0	0	0	0	0
AG8	7	7	0	0	0	0	0	0	0	0	0
AG9	13	7	0	0	0	0	0	0	0	0	0
AG10	0	3	0	0	0	0	0	0	0	0	0
AG11	0	7	0	0	0	0	0	0	0	0	0
AG12	0	7	0	0	0	0	0	0	0	0	0

Table V. *Comparison of ELISA reactivity in acute exacerbated and stable IPF*

Sample	Case No.	Ag (Designation) AG1	AG2	AG3	AG4	AG5	AG6	AG7	AG8	AG9	AG10	AG11	AG12
Acute exacerbation of IPF[a]													
Serum	10	47%[a]	40%[a]	33%[a]	27%[a]	20%[a]	13%	7%	7%	7%	0%	0%	0%
Mean OD 405 nm		1.73	1.57	0.98	1.06	0.54	0.52	0.46	0.44	0.52	0.56	0.49	0.43
SD 405 nm		1.46	1.36	0.82	0.65	0.36	0.40	0.10	0.05	0.08	0.06	0.12	0.15
Max. OD 405 nm		3.98	3.58	1.99	2.05	0.91	1.02	0.96	0.98	0.94	0.58	0.51	0.52
BAL fluid		53%[a]	47%[a]	40%[a]	33%[a]	27%[a]	13%	7%	7%	13%	0%	0%	0%
Mean OD 405 nm		1.83	1.75	1.52	0.86	0.55	0.56	0.58	0.44	0.49	0.56	0.51	0.46
SD 405 nm		1.34	1.46	0.64	0.72	0.44	0.42	0.12	0.15	0.05	0.04	0.13	0.16
Max. OD 405 nm		4.16	3.88	2.04	2.45	1.01	0.98	1.02	0.54	0.95	0.89	0.93	0.54
Stable IPF													
Serum	30	7%	10%	7%	3%	3%	10%	7%	7%	7%	3%	3%	7%
Mean OD 405 nm		0.43	0.50	0.38	0.45	0.41	0.42	0.42	0.48	0.52	0.36	0.48	0.55
SD 40 5nm		0.18	0.17	0.32	0.10	0.19	0.25	0.06	0.12	0.10	0.08	0.14	0.21
Max. OD 405 nm		0.98	0.92	0.89	0.92	0.88	0.87	0.93	0.94	0.98	0.88	0.94	0.96
BAL fluid		10%	7%	7%	3%	3%	13%	10%	7%	7%	3%	7%	7%
Mean OD 405 nm		0.53	0.57	0.46	0.42	0.53	0.39	0.38	0.52	0.44	0.49	0.46	0.52
SD 405 nm		0.18	0.15	0.18	0.09	0.18	0.12	0.28	0.10	0.08	0.06	0.18	0.21
Max. OD 405 nm		1.02	0.94	0.90	0.93	1.08	0.98	0.92	0.98	0.94	0.91	0.91	0.98

[a] The serum and BAL fluid Ab levels of annexin 1 (AG1), Bax inhibitor 1 (AG2), cytochrome c oxidase subunit 5a (AG3), heme oxygenase 1 (AG4), and phosphoglycerate kinase 1 (AG5) were significantly higher in cases of acute exacerbation of IPF than in stable IPF.

Sequencing Core kit. full-length annexin 1 was expressed in *E. coli* (M15 cells) using TAGZyme (Qiagen). The induction of recombinant protein synthesis, subsequent purification on Ni-NTA spin colums (Qiagen), and the complete removal of N-terminal His tags were conducted as instructed by the manufacture. Purified recombinant annexin 1 was incubated with human leukocyte elastase (Sigma-Aldrich) at a final concentration of 0.3 U/ml in reaction buffer (30). After electrophoresis of full-length annexin 1 and elastase-cleaved annexin 1 (each 25 μg protein), the proteins were electrotransferred to a nylon membrane and probed with sera of IPF patients (15 acute exacerbation patients, 30 stable patients) and non-IPF patients (90 patients with interstitial pneumonia related to collagen vascular disease, 30 patients with pulmonary sarcoidosis, 10 patients with chronic eosinophilic pneumonia, 10 patients with HP, and 40 normal volunteers).

Statistical analysis

The Mann-Whitney *U* test was used to compare the levels of Abs, CD4-positive T cell responses in BAL fluid, and in vitro assay of lymph node cells. p values of <0.05 were considered significant in the analysis.

Results

BAL profile

The median recovery rate of BAL samples from 15 acute exacerbated IPF cases was 54.7% (range, 37.6–67.2%). The cytological profile of BAL samples derived from cases of acute exacerbated IPF shows an increase in total cell numbers and marked neutrophilia (8–48%) compared with healthy control subjects (Tables I and III). BAL fluids obtained from all 15 acute exacerbation cases were negative for cultures of bacteria and fungi, and they showed negative results for PCR analysis of *Pneumocystis carinii* and cytomegalovirus.

SEREX analysis of patients with IPF

To determine the efficiency of the SEREX technique, we randomly picked up 1000 phagemids submitted to in vivo excision of the pBluescript plasmid. PCR analysis using primers that annealed to the T3 and T7 promoter regions flanking the multiple cloning site in the ZAP Express vector showed a range of cDNA inserts sizes from 200 to 7000 bp, with an average of ~2500 bp of these 1000 plasmids. The efficiencies of our SEREX technique for the generation of small protein Ags <360 bp (120 amino acids) and Ags larger than 1500 bp (500 amino acids) were ~1% and ~72%, respectively. Approximately 2.0×10^6 recombinant clones of a cDNA library derived from A549 cells were screened by 45 individual sera from patients suffering from acute exacerbation of IPF and stable IPF. Forty-nine positive clones representing 12 different known genes were detected. Table II summarizes the characteristics of the 12 genes identified by SEREX analysis of IPF patients. In acute exacerbation of IPF cases, the most frequently isolated genes were annexin 1 and Bax inhibitor 1, comprising 7 of 15 cases (47%) and 5 of 15 cases (33%), respectively. Another three Abs (cytochrome *c* oxidase subunit 5a, heme oxygenase 1, and phosphoglycerate kinase 1) were more highly detected in acute exacerbation of IPF than in stable IPF with frequencies of 3 of 15 cases (20%) to 4 of 15 cases (27%).

Survey of sera and BAL samples for Abs to the panel of recombinant autoantigens

The recombinant protein of cytochrome *c* oxidase subunit 5a represents full-length products, whereas the other 11 recombinant autoantigens represent almost full-length products (Table II). Table IV shows the reactivity to the 12 recombinant autoantigens of sera and BAL samples from patients with IPF, patients with other respiratory diseases, and healthy volunteers. Our study shows that Abs to annexin 1 were detected in 47% (7 of 15 cases) and 53% (8

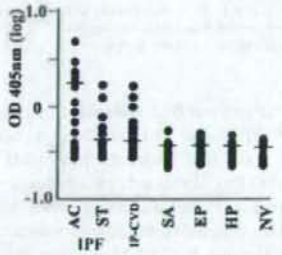

FIGURE 1. Serum levels of anti-annexin 1 Abs to the 6Xhistidine tag protein. Serum from patients with acute exacerbation (AE) and stable (ST) IPF, IP-CVD, pulmonary sarcoidosis (SA), eosinophilic pneumonia (EP), hypersensitivity pneumonitis (HP), and normal volunteer (NV) were examined. Horizontal bars indicate the mean values.

Table VI. *Identical TCR Vβ genes from first BAL/VATS biopsies and subsequent BAL samples from patients with acute exacerbation of IPF*

Case No. Clones	Incidence Rate* First Materials	Incidence Rate* Subsequent BAL	Junctional Sequence V	N-D-N	J	
1	1st BAL	2nd BAL				
1-1			C A S S Q	D Y V Q L A K S	E A F F	
	4/20	8/20	V3-1 TGTGCCAGCAGCCAA	GACTATGTTCAACTAGCTAAATCT	GAAGCTTTCTTT	J1-1
1-2			C A S S	P E A G G	E T Q Y F	
	3/20	4/20	V5-5 TGTGCCAGCAGC	CCAGAAGCGGGAGGT	GAGACCCAGTACTTC	J2-5
1-3			C A S S V	A L L E G	L F F	
	4/20	5/20	V9 TGTGCCAGCAGCGTA	GCCCTACTAGAGGGG	CTGTTTTTT	J2-2
2	1st BAL	2nd BAL				
2-1			C A S S Y	S A M V T S F	E Q F F	
	4/20	5/20	V6-2 TGTGCCAGCAGTTAC	TCAGCCATGGTAACTAGCTTC	GAGCAGTTCTTC	J2-1
3	1st BAL	2nd BAL				
3-1			C A S S Q	E G H Q T	V L T F	
	5/20	7/20	V14 TGTGCCAGCAGCCAA	GAGGGACACCAGACC	GTCCTGACTTTC	J2-6
3-2			C A T S R	E L Q G D T	G E L F F	
	3/20	3/20	V15 TGTGCCACCAGCAGA	GAGCTTCAGGGGGATACC	GGGGAGCTGTTTTTT	J1-2
3-3			C A S S V	A F L T V G C	S G N T I Y F	
	3/20	4/20	V9 TGTGCCAGCAGCGTA	GCCTTCAACCTCACAGGGTGT	TCTGGAAACACCATATATTTT	J1-3
4	1st BAL	2nd BAL				
4-1			C A S S Q	E G H Q T	V L T F	
	5/20	6/20	V14 TGTGCCAGCAGCCAA	GAGGGACACCAGACC	GTCCTGACTTTC	J2-6
4-2			C A S S L	A S L S I	G Y T F G	
	4/20	4/20	V7-8 TGTGCCAGCAGCTTA	GCTAGCCTAAGTATA	GGCTACACCTTCGGT	J1-2
4-3			C A S S V	A F L T V G C	N T I Y F	
	3/20	4/20	V9 TGTGCCAGCAGCGTA	GCCTTCAACCTCACAGGGTGT	AACACCATATATTTT	J1-3
5	1st BAL	2nd BAL				
5-1			C A S S Q	E Y T S T V Q	S P L H F	
	4/20	5/20	V4-3 TGTGCCAGCAGCCAA	GAATACACCAGCACCGTGCAA	TCACCCCTCCACTTT	J1-6
5-2			C A R S L	E F A F K T G Y	K L F F G	
	4/20	4/20	V5-3 TGTGCCAGAAGCTTA	GAATTTGCCTTCAAAACAGGGTAT	AAACTGTTTTTTGGC	J1-4
6	VATS	BAL				
6-1			C A S S L	L R L S G	Y N E Q F F	
	6/20	8/20	V12-3 TGTGCCAGCAGCTTA	CTACGACTGTCGGGG	TACAATGAGCAGTTCTTC	J2-1
6-2			C A S S E	V S D A G	A F F	
	4/20	4/20	V2 TGTGCCAGCAGCGAA	GTTTCGGACGCGGGG	GCTTTCTTT	J1-1
7	VATS	BAL				
7-1			C A S S I	Q S G R C I	S P L H F	
	6/20	4/20	V19 TGTGCCAGCAGCATT	CAACCGGGACGTTGTATA	TCACCCCTCCACTTT	J1-6
8	1st BAL	2nd BAL				
8-1			C A S S E	Y V P T D	K N I Q Y F	
	5/20	4/20	V10-2 TGTGCCAGCAGCGAA	TATGTCCCCACAGAC	AAAAACATTCAGTACTTC	J2-4
8-2			C S A R	L A Q G	T Q Y F	
	5/20	6/20	V20-1 TGTAGCGCCGAA	TTAGCCCAGGGT	ACGCAGTATTTT	J2-3
8-3			C A S S L	L R W A P	G E L F F	
	3/20	4/20	V7-2 TGTGCCAGCAGCTTA	CTGCGGTGGGCCCCG	GGGGAGCTGTTTTTT	J2-2
9	1st BAL	2nd BAL				
9-1			C A S S P	L T G V F T K	T E A F F	
	5/20	6/20	V18 TGTGCCAGCAGCCCC	CTAACGGGAGTCTTCACAAAG	ACTGAAGCTTTCTTT	J1-1
9-2			C A S S Q	Y R R S N G	Q Y F	
	4/20	4/20	V3-1 TGTGCCAGCAGCCAA	TATCGCCGATCCAATGGG	CAGTACTTC	J2-4
10	VATS	BAL				
10-1			C A S S Q	K A P G N R	N Q P Q H F	
	5/20	4/20	V4-3 TGTGCCAGCAGCCAA	AAAGCACCGGGAAATAGG	AATCAGCCCCAGCATTTT	J1-5

* In all 10 cases (cases 1–10), some identical TCR Vβ genes were detected by sequencing analysis of the RT-PCR product of the first BAL fluid or VATS materials and sequential BAL samples with frequencies ranging from 3 of 20 to 8 of 20 clones. The results of sequencing are presented as the incidence rates of the predominant sequences out of the total number of vector clones analyzed.

of 15 cases) of the sera and BAL materials from patients with acute exacerbation of IPF, and >7% (2 of 30 cases) and 10% (3 of 30 cases) of the sera and BAL materials from stable IPF patients.

Four other Ags (Bax inhibitor 1, cytochrome *c* oxidase subunit 5a, heme oxygenase 1, and phosphoglycerate kinase 1) reacted with sera and BAL materials from patients with acute exacerbation of IPF with frequencies 20–33% higher than those of stable IPF patients. No specific Ab reactivity to annexin 1 was detected in either the sera or BAL materials from 40 normal volunteers and non-IPF subjects except for 10% reactivity in sera samples from patients with RA and SLE-related interstitial pneumonia. The 11 other Abs were also more frequently detected in both serum and BAL samples from IPF patients (acute exacerbation and/or stable cases) than other subjects and control volunteers, although a few non-IPF subjects showed reactivity to some Ags.

Comparison of Ab levels in serum and BAL samples between acute exacerbation of IPF and stable IPF

The serum and BAL fluid Ab levels of annexin 1, Bax inhibitor 1, cytochrome *c* oxidase subunit 5a, heme oxygenase 1, and phosphoglycerate kinase 1 were significantly higher in cases of acute exacerbation of IPF than in stable IPF (Table V). The data of

Table VII. *Homology between identical TCR Vβ genes and T cell epitopes predicted by the TEPITOPE program*

Case No.	T Cell Clone	TCR Vβ CDR3 Regions[a] Peptides of Ags[a] (position)	Ag Identified by SEREX	T Cell Epitopes Predicted by the TEPITOPE Program	
				Residual Nos.[b]	MHC Allele
1	1-1	ASSQDYVQLAKSAF			
		NEEQEYVQTVKSSKG (15–29)	Annexin 1	21–29,[b] 285–293	DRB1*0404
	1-3	CASSVALLEGLFF			
		AAGSVILLENLRF (111–123)	Phosphoglycerate kinase 1	115–123[b]	DRB1*0404
				115–123,[b] 220–228, 242–252	DRB1*0410
2	2-1	CASSYSAKVTSEQFF			
		AAGAYVHRVTSFIQAG (42–57)	Bax inhibitor 1	46–54,[b] 214–222	DRB1*0802
				NA	DRB1*1401
3	3-1	ASSQEGHQTVLTF			
		NEEQEYVQTVKSS (15–27)	Annexin 1	20–28,[b] 47–55, 285–293	DRB1*1307
				317–325, 334–342	
				217–225, 314–322	DRB1*1502
	3-3	CASSVAFLTVGCSGNTIYF			
		GTDEVKFLTVLCSRNRNHL (186–204)	Annexin 4	75–85, 190–198,[b] 211–219	DRB1*1307
				79–87, 139–147, 190–198,[b] 238–246, 254–262	DRB1*1502
5	5-1	ASSQEYTSTVQSPLH			
		NEEQEYVQTVKSSKG (15–29)	Annexin 1	21–29,[b] 286–294, 297–305, 314–326	DRB1*0101
				217–225, 314–322	DRB1*1501
	5-2	LEFAFKTGYKLFFG			
		AGFAFLTGVGLGPA (89–102)	Bax inhibitor 1	39–54, 91–99,[b] 140–148	DRB1*0101
				66–74, 177–191	DRB1*1501
7	7-1	ASSIQSGRCTSPL			
		AVAIQSVRCYEHG (32–44)	Cytochrome c oxidase subunit 5a	NA[c]	DRB1*0901
				NA	DRB1*1001
8	8-1	CASSEYVPTDKNI			
		NEEQEYVQTVKSS (15–27)	Annexin 1	NA	DRB1*0403
				106–115, 174–182, 219–227, 295–304	DRB1*1502

[a] Identical amino acid residues in the CDR3 region of identical CD4-positive lymphocytes clones and autoantigens derived from SEREX analysis are underlined.
[b] The positions of identical amino acids residues included in the T cell epitopes predicted by TEPITOPE program are demonstrated.
[c] NA, Not applicable.

serum Ab levels of annexin 1 were also shown as a log titer graph (Fig. 1). In contrast, the levels of the seven other Abs did not differ between acute exacerbation of IPF and stable IPF, or they were lower in stable IPF than in acute exacerbation of IPF cases.

Sequence analysis of the TCR Vβ gene rearrangements of IPF

All 15 acute exacerbation of IPF cases showed some predominant TCR Vβ repertoires of CD4-positive cells on Southern blot analysis of BAL samples (Table I). In all 10 patients (cases 1–10), some identical TCR Vβ genes were detected by sequencing analysis of the RT-PCR product of the first BAL fluid or VATS materials and sequential BAL samples. The results of sequencing are presented as the incidence rates of the predominant sequences out of the total number of vector clones analyzed. Some identical rearrangements of TCR Vβ genes existed, with frequencies ranging from 3 of 20 to 8 of 20 clones in both the first BAL or VATS samples and subsequent samples (Table VI).

Identical CDR3 of TCR Vβ clones in sequential samples and TEPITOPE analysis

We determined HLA-DR Ags in all 15 acute exacerbation of IPF cases (Table I). In 6 patients (cases 1, 2, 3, 5, 7, and 8) in which identical CDR3 regions of TCR Vβ clones in sequential samples showed high homology with Ags detected by SEREX analysis, 8 of 12 HLA-DRB Ags could be analyzed by the TEPITOPE method (Table VII). In acute exacerbation of IPF cases, including those with HLA-DRB Ags, all except one (clone 8-1) CDR3 region of identical clones were included in the epitopes of the autoantigens predicted by TEPITOPE analysis. The CDR3 regions of identical TCR Vβ genes (clones 1-1, 3-1, 5-1, and 8-1) show high homology with the same portion (residues 18–26) of annexin 1. In contrast, CDR3 regions of TCR Vβ genes (clones 2-1 and 5-2) show homology with the different portions of Bax inhibitor 1 genes. Focus was thus placed on annexin 1 for further studies of CD4-positive T cell responses in BAL fluid.

Western blot analysis of annexin 1 in BAL samples from IPF patients and non-IPF patients

With the use of BAL fluid proteins, annexin 1 was detected in all 15 cases of acute exacerbation of IPF. Western blot analysis showed full-length (36 kDa) and/or a cleaved form (33 kDa) of annexin 1 in BAL fluid proteins in cases of acute exacerbation of IPF. Typical examples of the analyses are shown in Fig. 2*A*. It appeared that some BAL fluid samples from patients with acute exacerbation of IPF (cases 1, 3, 5, 7, 8, and 10), which contained ~20% or more neutrophils on the differential cell count (Table I), included large amounts of the cleaved form of annexin 1 equal to

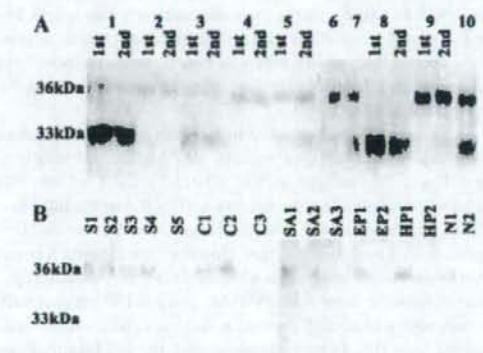

FIGURE 2. Western blot analysis of annexin 1 in BAL materials from patients with acute exacerbation of IPF (*A*), stable IPF, and non-IPF (*B*). *A*, Numbers above the lanes correspond to the case numbers of acute exacerbation of IPF in Table I. 1st and 2nd represents 1st BAL and 2nd BAL materials. *B*, Each lane represents typical BAL samples from individual subject. S1–S5, stable IPF; C1–C3, collagen vascular disease; SA1–SA3, pulmonary sarcoidosis; EP1 and EP2, eosinophilic pneumonia; HP1 and HP2, hypersensitivity pneumonitis; N1 and N2, normal volunteers.

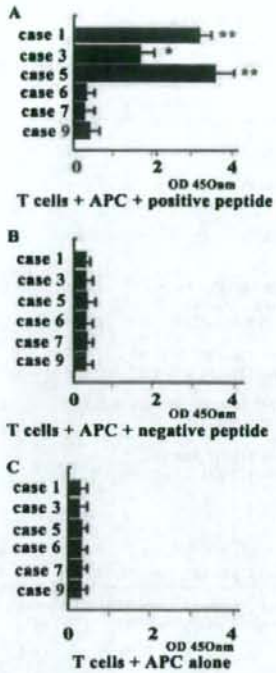

FIGURE 3. BrdU assay response of CD4-positive T cells to N-terminal peptides of annexin 1 in patients with acute exacerbation of IPF cases. Values represent means + SD of triplicate cultures. *A*, T cells + APC + positive peptide (QEYVQTVKS). Annexin 1-positive peptide induced marked proliferative responses of CD4-positive T cells with APC (alveolar macrophages) in three patients (cases 1, 3, and 5) with high titers of anti-annexin 1 Abs compared with another three patients (cases 6, 7, and 9). Asterisks indicate values significantly different from other cases or peptides (*, $p < 0.05$; **, $p < 0.01$). *B*, T cells + APC + negative peptide. *C*, T cells + APC alone. Annexin 1-negative peptide (DARALYEAG) or no peptide induced proliferative responses of CD4-positive T cells in none of all six patients.

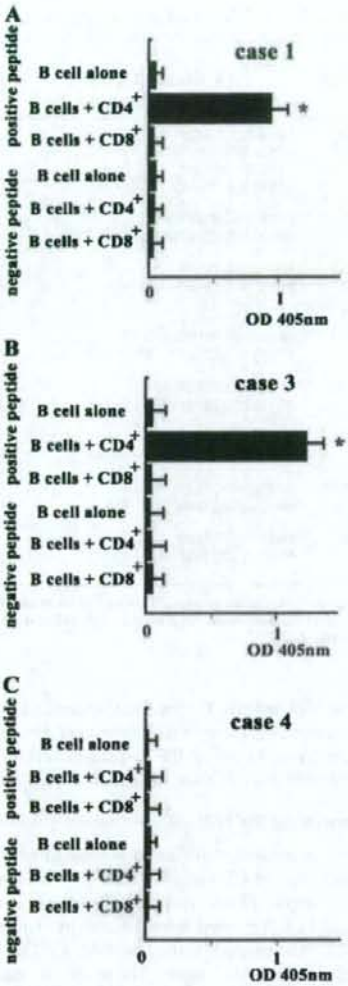

FIGURE 4. In vitro anti-annexin 1 Ab production in lymph node cell cultures in response to annexin 1 peptides. Lymph node cells from patients with acute exacerbation of IPF cases were cultured with annexin 1-positive (QEYVQTVKS) or -negative (DARALYEAG) peptides for 10 days, and anti-annexin 1 Ab levels were measured by ELISA. Values represent means + SD of triplicate cultures. Two patients (cases 1 (*A*) and 3 (*B*)) displayed high titers of annexin 1 Abs and the other patient (case 4 (*C*)) was negative for annexin 1 Ab. Asterisks indicate values significantly different from other cases or peptides (*, $p < 0.01$).

or larger than the amount of the full length of annexin 1. In case 5, the first BAL fluid protein demonstrated only full-length annexin 1, with 8% neutrophils on the differential cell count. In contrast, the second BAL fluid samples of case 5 showed a short form as well as the long form of annexin 1, with 28% neutrophils on the differential cell count.

In contrast, in 30 BAL fluid samples from stable IPF patients and 90 patients with collagen vascular disease, the full length of annexin 1 was also present in 5 of 30 (16%) and 6 of 90 (7%) samples, respectively. The six patients with collagen vascular disease were composed of one PM/DM patient, one Ssc patient, two RA patients, and two SLE patients. However, the cleaved form of annexin 1 was absent in all cases with stable IPF and with collagen vascular disease. In other non-IPF BAL samples (30 patients with pulmonary sarcoidosis, 10 patients with eosinophilic pneumonia, 10 patients with HP, 40 normal volunteers), the full length of annexin 1 was only barely detected. Typical examples of patients with stable IPF and non-IPF are shown in Fig. 2*B*.

T cell responses in BAL fluid to N-terminal annexin 1 peptides

N-terminal annexin 1-positive peptides induced marked proliferative responses of CD4-positive T cells in three patients (cases 1, 3, and 5) with high titers of annexin 1 Abs, compared with three other patients (cases 6, 7, and 9) ($p < 0.05$; Fig. 3). Annexin 1-negative peptides or no peptide induced proliferative responses of CD4-positive T cells in none of all six cases.

In vitro anti-annexin 1 Ab production in response to annexin 1 peptide

The effect of N-terminal-positive peptides of annexin 1 compared with negative peptides for B cell autoreactivity was examined in three cases (Fig. 4). B cells and $CD4^+$ T cell subsets from two acute exacerbation IPF patients (cases 1 and 3) with high titers of annexin 1 Abs in their serum and BAL produced high levels of anti-annexin 1 Abs in response to N-terminal annexin 1-positive

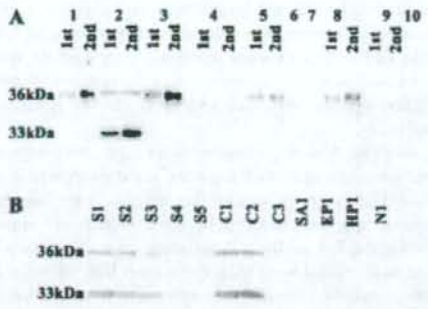

FIGURE 5. Western blot analysis of full-length and elastase-cleaved annexin 1 probed with sera from patients with acute exacerbation of IPF (*A*), stable IPF, and non-IPF (*B*). *A*, The numbers above the lanes correspond to the case numbers of acute exacerbation of IPF in Table I. 1st and 2nd represent 1st BAL and 2nd BAL materials. *B*, Each lane represents typical BAL samples from an individual subject. S1–S5, stable IPF; C1–C3, collagen vascular disease; SA1, pulmonary sarcoidosis; EP1, eosinophilic pneumonia; HP1, hypersensitivity pneumonitis; N1, normal volunteer.

peptides. In contrast, only B cells or B cells and $CD8^+$ T cell subsets from two such cases did not produce anti-annexin 1 Ab. In the other case (case 4) negative for anti-annexin 1 Abs in his serum and BAL, none of the lymph node cell culture supernatants in response to annexin 1-positive or -negative peptides contained a high amount of anti-annexin 1 Abs.

Western blot analysis of full-length and elastase-cleaved annexin 1 probed with sera from IPF and non-IPF patients

To determine whether anti-annexin 1 Ab preferentially binds to the N-terminal portion of annexin 1 cleaved by neutrophil elastase, we analyzed Western blots of full-length and elastase-cleaved annexin 1 probed with sera from IPF and non-IPF patients. With the use of sera, blots were able to bind to the full-length and/or the cleaved form of annexin 1 in 7 of 15 cases with acute exacerbation of IPF. Typical examples of the analyses are shown in Fig. 5.

Four patients (cases 1, 3, 5, and 8) with acute exacerbation of IPF demonstrated that their sera only bound to the full length of annexin 1 without binding to the cleaved one. This result suggested that the anti-annexin 1 Abs in these four cases bound the N-terminal portion of annexin 1, which did not exist in the cleaved form. In contrast, in 30 patients with stable IPF and 90 patients with collagen vascular disease, 3 of 30 (10%) patients and 2 (1 RA patient and 1 SLE patient) of 90 (2%) patients demonstrated that their sera bound to both the full-length and the cleaved form of annexin 1, respectively. In other non-IPF BAL samples (30 patients with pulmonary sarcoidosis, 10 patients with eosinophilic pneumonia, 10 patients with HP, 40 normal volunteers), sera did not bind to either the full-length or the cleaved form of annexin 1.

Discussion

This study initiates a survey of the humoral immune response related to the pulmonary epithelial pathology of patients with acute exacerbated or stable IPF to 12 autoantigens identified by SEREX methods using a cDNA phage library of type II alveolar cell carcinoma (A549) cell lines. In a survey of serum and BAL samples for Abs to the panel of recombinant autoantigens identified by SEREX analysis, five (annexin 1, Bax inhibitor 1, cytochrome *c* oxidase subunit 5a, heme oxygenase 1, phosphoglycerate kinase 1) Abs were identified as novel candidates for autoantigens in acute exacerbation of IPF using the SEREX. In particular, several findings in the present study suggest that annexin 1 is involved not only in Ab production, but also in CD4-positive T cell responses derived from BAL samples in acute exacerbated IPF patients. Western blotting analysis and CD4-positive T cell responses of BAL samples demonstrated that the N-terminal portion of annexin 1 might play an important role in the immune pathophysiology of acute exacerbated IPF patients.

Considering that the efficiency of our SEREX technique for the generation of small protein (<120 amino acids) was low (~1%) and that the average insert size was ~2500 bp, our technique was not efficient for certain proteins and did not skew the identification of Ags by patients' sera. By applying the SEREX approach using the serum of patients with acute exacerbation of IPF, we could detect nine Abs with frequencies ranging from 7 of 15 (47%) to 1 of 15 (7%). Three more Abs were found with frequencies ranging from 2 of 30 (7%) to 1 of 30 (3%) by the SEREX analysis using serum from patients with stable IPF. Another report involving SEREX analysis using expressed cDNA libraries derived from another tumor cell line (AB1) showed three Abs (ATS, IGBP1, brain EST) in IPF patients (31). Anti-cytokeratin 8 Abs have been reported in sera from patients with IPF by Western blotting analysis (6). In our report, we detected anti-cytokeratin 8 Abs in 2 of 30 (7%) patients with stable IPF, but not in patients with acute exacerbation of IPF. The results of the present study demonstrate that five Abs (annexin 1, Bax inhibitor 1, cytochrome *c* oxidase subunit 5a, heme oxygenase 1, phosphoglycerate kinase 1) are present at frequencies from 3 of 15(20%) to 7 of 15 (47%) in serum from patients with acute exacerbation of IPF, but not from patients with stable IPF.

Because we wanted to determine the relevance of the Abs detected by the SEREX method as clinical markers of IPF, we conducted ELISA using 12 recombinant autoantigens. Serum levels of all 12 Abs were higher in patients with IPF than in other groups. A minority of non-IPF subjects exceptionally demonstrated slightly elevated Ab titers. The levels of Abs to most of our 12 autoantigens in BAL samples were preferentially elevated in patients with IPF (Table IV). Only a few non-IPF patients studied exhibited elevated Ab levels in their serum and BAL samples. Because local inflammation is remarkably different from the systemic immune response, BAL samples are superior to serum as a source of Abs in terms of monitoring local pulmonary immunological reactions. Measurement of Abs to our 12 autoantigens in BAL samples could be a specific and sensitive means of identifying individuals with IPF. In our study, patients with acute exacerbation of IPF exhibited significantly higher levels of serum and BAL fluid Abs to 5 (annexin 1, Bax inhibitor 1, cytochrome *c* oxidase subunit 5a, heme oxygenase 1, phosphoglycerate kinase 1) of the 12 autoantigens identified by SEREX analysis (Table V). Interestingly, three of these five Ags are related to apoptosis. These autoantibodies are unlikely to be the primary cause of tissue damage, although they might reflect prominent apoptosis of alveolar epithelial cells in cases of acute exacerbation of IPF. Because carcinoma cell lines are by their nature going to be altered from the native type II cells, and they are more than likely overrepresented with proteins regulating apoptosis, the A549 cell line would be suitable for our SEREX analysis to detect Abs related to apoptosis.

One difference between apoptotic and necrotic death is that programmed cell death results in the ordered fragmentation of cells, leading to rapid phagocytosis by neighboring cells and/or professional phagocytes without cell activation and inflammation (32). Apoptosis is important in the remodeling of tissues during repair. However, during apoptosis, the cell membrane forms cytoplasmic

blebs, some of which are shed as apoptotic bodies, and a number of autoantigens are located at the cell surface or within the apoptotic blebs (33). It has been reported that normal mice injected with syngeneic apoptotic thymocytes develop autoantibodies, whereas similar mice immunized with nonapoptotic syngeneic splenocytes generally do not develop autoantibodies (34). Moreover, cultured keratinocytes exposed to UV B/UV A irradiation (known apoptotic stimulus) demonstrate enhanced binding of autoantibodies directed against Sm, RNP, Ro, and La to the cell-surface membrane (35). Such findings indicate that the handling of apoptotic cells is not always silent and that apoptotic cells may serve as reservoirs of autoantigens. Accumulating data suggest that a breakdown in tolerance leading to the production of autoantibodies may be attributed to posttranslational modifications of autoantigens during apoptosis or cellular stress, resulting in the creation of neoepitopes to which the immune system has never been exposed (36). Although it remains uncertain what causes acute exacerbation of IPF, the pathologic findings of autopsy specimens with respect to acute exacerbation of IPF demonstrate that IL-1β and TNF-α are strongly positive in alveolar macrophages and type II pneumocytes. Such proinflammatory cytokines may enhance the apoptosis of type II pneumocytes. The elevated levels of some Abs to Ags related to apoptosis in acute exacerbation may reflect the aberrant antigenicity of apoptotic type II pneumocytes. Note that apoptotic cells administered intratracheally directly into the lungs of rats are reported to induce secondary apoptosis by apoptotic cell instillation, leading to pulmonary fibrosis (37).

Annexin I is included among the autoantigens detected in this study. Annexins comprise a group of calcium-dependent phospholipid-binding proteins. The calcium- and phospholipid-binding sites of most annexins are located in four repeated and highly conserved regions, each of which contains ~70 amino acids. Although multiple functions of annexins have been suggested, including activities in exocytosis, signal transduction, antiinflammation, anticoagulation, and calcium channel regulation, it is possible that each of these annexin functions is tissue-specific. The lung is rich in annexins, and annexin I appears to be the most abundant protein among the annexin family of proteins in the mammalian lung, where it exists in alveolar epithelial type II cells and in alveolar macrophages. Annexin I was discovered >20 years ago as a protein that mediates the antiinflammatory action of glucocorticoids. Two effects have been proposed to explain how exogenously applied annexin I could interfere with inflammatory processes. The first effect involves the regulation of eicosanoid production. Annexin I inhibits phospholipase A_2, the first enzyme in the metabolism of eicosanoids, and it has been proposed that this inhibition and the resulting decrease in arachidonic acid release are the basis of the antiinflammatory effect (38). It has been reported that cytosolic phospholipase A_2 plays a pivotal role in the pathogenesis of pulmonary fibrosis, and that disruption of the gene encoding cytosolic phospholipase A_2 significantly attenuates pulmonary fibrosis (39). 2) The second effect relates to a reduction in the recruitment of blood-borne cells into the surrounding tissues (40). Passive immunization with antiannexin I Abs abrogates the inhibitory glucocorticoid effect on neutrophil extravasation and leads to an exacerbation of inflammatory diseases. Annexin I and N-terminal annexin I peptides (position 19–25: EYVQTVK) significantly interfere with neutrophil transmigration (41). It has been reported that the annexin I N-terminal peptide can bind to the formyl peptide receptor on neutrophils and prevent transendothelial extravasation, a finding that supports the antiinflammatory role of annexin I. Considering that annexin I may be an endogenous ligand mediating the engulfment of apoptotic cells, and that the silencing of the annexin I protein by small interfering RNA results in defective tethering and engulfment of apoptotic cells, Abs against annexin I in patients with acute exacerbation of IPF may block the cell surface-exposed annexin I presented on apoptotic cell surfaces, leading to the prevention of the removal of apoptotic cells. This, in turn, may accelerate the further generation of autoantibodies.

Bax inhibitor 1 is an antiapoptotic protein containing several transmembrane domains that localizes to the endoplasmic reticulum (ER). The overexpression of Bax inhibitor 1 provides protection against apoptosis induced by some stimuli in mammalian cells, while the Bax inhibitor 1 antisense gene can promote apoptosis of some tumor lines (42). Cells from Bax inhibitor 1-deficient mice, including fibroblasts, display selective hypersensitivity to apoptosis induced by ER stress agents, but not to stimulators of the mitochondrial or TNF/Fas death receptor apoptosis pathways (43). Bax inhibitor 1 appears to block the transmission of death signals from damaged ER/Golgi to mitochondria. It has been reported that the expressions of caspases-8, -9, and -3, as well as cytochrome *c* release from mitochondria, are increased in the lung tissues of IPF compared with normal lung parenchyma (44). ER stress independently triggers caspase-8 activation, resulting in cytochrome *c*/caspase-9 activation. Although the role of ER stress in IPF has not been extensively studied, ER stress such as hypoxia might play some role in the pathogenesis of the acute exacerbation of IPF. Further examination of ER stress in acute exacerbation of IPF is necessary to clarify this possibility.

After establishing autoantibodies in patients with acute exacerbation of IPF, we analyzed whether these Abs recognize Ags that elicit T cell responses. Because the nonspecific recruitment of T cells may mask disease-related T cell populations, we separated CD4-positive subsets and analyzed TCR Vβ genes to reduce the dilution effect of CD4-negative T cell populations. Previously it was reported that the TCR Vβ repertoire shows some predominant oligoclonal T cell expansions in BAL samples from IPF patients (17). These findings support the hypothesis that CD4-positive T cells in BAL fluid of patients with IPF would be induced by Ags on APCs, and that T cells in pulmonary lesions might expand by Ag stimulation in the context of HLA, rather than stimulation by superantigens. To determine whether oligoclonal CD4-positive lymphocyte expansions persist over time, we had the opportunity to study first BAL or VATS materials and sequential BAL samples. We were able to show some identical TCR Vβ rearrangements in the first and second biopsy materials obtained from patients with acute exacerbation of IPF (cases 1–10). The oligoclonal expansions of CD4-positive lymphocytes with identical CDR3 regions on their TCR Vβ genes existed over time, suggesting that continuous inflammation due to the same Ag-driven stimulation by the recognition of a restricted epitope on the major MHC through TCR occurs in the alveoli of patients with acute exacerbation of IPF. Such immunodominance may be dictated by Ag-processing mechanisms, by intermolecular competition for MHC binding, and by the existence of a biased T cell repertoire. Ags that react with CD4-positive lymphocytes with identical CDR3 regions on their TCR Vβ genes might play some roles in IPF immunology and might reflect immunological reactions at the site of the alveoli in patients with acute exacerbation of IPF.

The binding groove in HLA-II molecules has open ends and therefore accommodates peptides of varying lengths (12–28 amino acids) that bind in an extended conformation. TEPITOPE analysis has been designed to enable the computational identification of promiscuous and allele-specific HLA-DR ligands (45). It was successfully used to identify HLA-DR ligands derived from tumors and endogenous proteins involved in autoimmune diseases (46). We used TEPITOPE analysis to investigate promiscuous HLA-DR

ligands of autoantigens related to IPF as defined by the SEREX approach. The identical CDR3 regions of TCR Vβ on CD4-positive lymphocytes from the BAL fluid of patients with acute exacerbation of IPF were compared with HLA-DR ligands in the same patients. Nine epitopes (clones 1-1, 1-3, 2-1, 3-1, 3-3, 5-1, 5-2, 7-1, and 8-1) of the CDR3 regions showed some homology with HLA-DR ligands in each case. Three clones (1-1, 3-1, and 5-1) from different IPF patients (cases 1, 3, and 5) recognized the same epitopes (position 18–26) of annexin 1, also included in the HLA-DR ligand epitopes of the same IPF patients predicted by TEPITOPE analysis (Table VII). These findings demonstrate the possibility that these autoantigens might play some immunological role in the lungs of patients with acute exacerbation of IPF.

The epitopes (position 18–26) of annexin 1 that recognized three clones from three different cases of acute exacerbation of IPF include an N-terminal annexin 1 motif (position 19–25: EYVQTVK) that has been reported to inhibit neutrophil extravasation (41). Western blot analysis of BAL fluid samples detected the 33-kDa annexin 1 breakdown product in patients with acute exacerbation of IPF whose BAL differential cell counts included relatively high percentages of neutrophils (Table I and Fig. 1), but not in BAL samples from patients with stable IPF or various other respiratory diseases (data not shown). Annexin 1 appears to be cleaved by neutrophil elastase at the N-terminal portion between Val^{36} and Ser^{37} to yield the 33-kDa protein (47). Considering the fact that this cleaved N-terminal portion includes an N-terminal annexin 1 peptide that interferes with neutrophil transmigration, these cleaved peptides might play some role in the pathogenesis of acute exacerbation of IPF. It has been reported that among BAL fluid samples from patients with interstitial lung diseases, some samples contained degraded annexin 1, and that the degradation on annexin 1 is associated with a relatively higher percentage of neutrophils in these samples (47). It has been reported that the cleavage of annexin 1 in its NH2-terminal region yields a truncated protein that exhibits catalytic properties distinct from those of the full-length protein (48). Analysis of CD4-positive responses of T cells from BAL samples revealed a CD4-positive T cell responses to N-terminal annexin 1 peptides (position 18–26: QEYVQTVKS) in BAL samples and found marked proliferative responses in patients with high titers of anti-annexin 1 Abs compared with other patients who were negative for anti-annexin 1 Abs. This N-terminal annexin 1 peptide (position 18–26: QEYVQTVKS) might play some role in the acute exacerbation of IPF. Although the exact biologic implications of N-terminal annexin 1 peptides in the development of acute exacerbation of IPF await further study, these results define autoantigens that might participate in the immunopathogenesis of acute exacerbation of IPF.

Acknowledgments

We thank Dr. Fuminobu Kuroda (Department of Respirology) and Dr. Fumio Nomura and Masayuki Ohyama (Department of Molecular Diagnosis) of Chiba University for skillful technical assistance.

Disclosures

The authors have no financial conflicts of interest.

References

1. Hunninghake, G. W., M. B. Zimmerman, D. A. Schwartz, T. E. King, Jr., J. Lynch, R. Hegele, J. Waldron, T. Colby, N. Muller, D. Lynch, et al. 2001. Utility of a lung biopsy for the diagnosis of idiopathic pulmonary fibrosis. *Am. J. Respir. Crit. Care Med.* 164: 193–196.
2. Kondoh, Y., H. Taniguchi, Y. Kawabata, K. Suzuki, and K. Takagi. 1993. Acute exacerbation in idiopathic pulmonary fibrosis: analysis of clinical and pathologic findings in three cases. *Chest* 103: 1808–1812.
3. Ambrosini, V., A. Cancellieri, M. Chilosi, M. Zompatori, R. Trisolini, L. Saragoni, and V. Poletti. 2003. Acute exacerbation of idiopathic pulmonary fibrosis: report of a series. *Eur. Respir. J.* 22: 821–826.
4. Wallace, W. A., S. N. Roberts, H. Caldwell, E. Thornton, A. P. Greening, D. Lamb, and S. E. Howie. 1994. Circulating antibodies to lung protein(s) in patients with cryptogenic fibrosing alveolitis. *Thorax* 49: 218–222.
5. Wallace, W. A., I. A. Schofield, D. Lamb, and S. E. Howie. 1994. Localisation of a pulmonary autoantigen in cryptogenic fibrosing alveolitis. *Thorax* 49: 1139–1145.
6. Dobashi, N., J. Fujita, Y. Ohtsuki, I. Yamadori, T. Yoshinouchi, T. Kamei, M. Tokuda, S. Hojo, and J. Takahara. 1998. Detection of anti-cytokeratin 8 antibody in the serum of patients with cryptogenic fibrosing alveolitis and pulmonary fibrosis associated with collagen vascular disorders. *Thorax* 53: 969–974.
7. Yu, W., K. J. Han, X. W. Pang, H. A. Vaughan, W. Qu, X. Y. Dong, J. R. Peng, H. T. Zhao, J. A. Rui, X. S. Leng, et al. 2002. Large scale identification of human hepatocellular carcinoma-associated antigens by autoantibodies. *J. Immunol.* 169: 1102–1109.
8. Eichmuller, S., D. Usener, R. Dummer, and A. Stein. 2001. Serological detection of cutaneous T-cell lymphoma-associated antigens. *Proc. Natl. Acad. Sci. USA* 98: 629–634.
9. Jeoung, D. I., E. B. Lee, S. Lee, Y. Lim, D. Y. Lee, J. Kim, H. Y. Kim, and Y. W. Song. 2002. Autoantibody to DNA binding protein B as a novel serological marker in systemic sclerosis. *Biochem. Biophys. Res. Commun.* 299: 549–554.
10. Jeoung, D., Y. Lim, E. B. Lee, S. Lee, H. Y. Kim, H. Lee, and Y. W. Song. 2004. Identification of autoantibody against poly(ADP-ribose) polymerase (PARP) fragment as a serological marker in systemic lupus erythematosus. *J. Autoimmun.* 22: 87–94.
11. Schmits, R., B. Kubuschok, S. Scuster, K. D. Preuss, and M. Pfreundschuh. 2002. Analysis of the B cell repertoire against autoantigens in patients with giant cell arthritis and polymyalgia rheumatica. *Clin. Exp. Immunol.* 127: 379–385.
12. Barbas-Filho, J. V., M. A. Ferreira, A. Sesso, R. A. Kairalla, C. R. Carvalho, and V. L. Capelozzi. 2001. Evidence of type II pneumocyte apoptosis in the pathogenesis of idiopathic pulmonary fibrosis (IPF)/usual interstitial pneumonia (UIP). *J. Clin. Pathol.* 54: 132–138.
13. Uhal, B. D., I. Joshi, W. F. Hughes, C. Ramos, A. Pardo, and M. Selman. 1998. Alveolar epithelial cell death adjacent to underlying myofibroblasts in advanced fibrotic human lung. *Am. J. Physiol.* 275: L1192–L1199.
14. Hagimoto, N., K. Kuwano, H. Miyazaki, R. Kunitake, M. Fujita, M. Kawasaki, Y. Kaneko, Y. Nomoto, and N. Hara. 1997. Induction of apoptosis and pulmonary fibrosis in mice in response to ligation of Fas antigen. *Am. J. Respir. Cell Mol. Biol.* 17: 272–278.
15. Lee, C. G., S. J. Cho, M. J. Kang, S. P. Chapoval, P. J. Lee, P. W. Noble, T. Yehualaeshet, B. Lu, R. A. Flavell, J. Milbrandt, et al. 2004. Early growth response gene 1-mediated apoptosis is essential for transforming growth factor β1-induced pulmonary fibrosis. *J. Exp. Med.* 200: 377–389.
16. Hagimoto, N., K. Kuwano, Y. Nomoto, R. Kunitake, and N. Hara. 1997. Apoptosis and expression of FAS/FAS ligand mRNA in bleomycin-induced pulmonary fibrosis in mice. *Am. J. Respir. Cell Mol. Biol.* 16: 91–101.
17. Shimizudani, N., H. Murata, H. Keino, S. Kojo, H. Nakamura, Y. Morishima, T. Sakamoto, M. Ohtsuka, K. Sekisawa, M. Sumida, et al. 2002. Conserved CDR3 region of T cell receptor BV gene in lymphocytes from bronchoalveolar lavage fluid of patients with idiopathic pulmonary fibrosis. *Clin. Exp. Immunol.* 129: 140–149.
18. Katchar, K., J. Wahlstrom, A. Eklund, and J. Grunewald. 2001. Highly activated T-cell receptor AV2S3$^+$CD4$^+$ lung T-cell expansions in pulmonary sarcoidosis. *Am. J. Respir. Crit. Care Med.* 163: 1540–1545.
19. Yamamoto, K., H. Sakoda, T. Nakajima, T. Kato, M. Okubo, M. Dohi, Y. Mizushima, and K. Ito. 1992. Accumulation of multiple T cell clonotypes in synovial lesions of patients with rheumatoid arthritis revealed by a novel clonality analysis. *Int. Immunol.* 4: 1219–1223.
20. Feng, X., T. Chuhjo, C. Sugimori, T. Kotani, X. Lu, A. Takami, H. Takamatsu, H. Yamazaki, and S. Nakao. 2004. Diazepam-binding inhibitor-related protein 1: a candidate autoantigen in acquired aplastic anemia patients harboring a minor population of paroxysmal nocturnal hemoglobinuria-type cells. *Blood* 104: 2425–2431.
21. Kita, H., Z. X. Lian, I. Van de Water, X. S. He, S. Matsumura, M. Kplan, V. Luketic, R. T. Coppel, A. A. Ansari, and M. E. Gershwin. 2002. Identification of HLA-A2-restricted CD8 cytotoxic T cell responses in primary biliary cirrhosis: T cell activation is augmented by immune complexes cross-presented by dendritic cells. *J. Exp. Med.* 195: 113–123.
22. Wucherpfennig, K. W., I. Catz, S. Hausmann, J. L. Strominger, L. Steinman, and K. G. Warren. 1997. Recognition of the immunodominant myelin basic protein peptide by autoantibodies and HLA-DR2-restricted T cell clones from multiple sclerosis patients: identity of key contact residues in the B-cell and T-cell epitopes. *J. Clin. Invest.* 100: 1114–1122.
23. King, T. E., Jr., U. Costabel, J. F. Cordier, G. A. DoPico, R. M. Bois, D. Lynch, J. P. Lynch, J. Myers, R. Panos, G. Raghu, et al. 2000. Idiopathic pulmonary fibrosis: diagnosis and treatment. *Am. J. Respir. Crit. Care Med.* 161: 646–664.
24. Akira, M., H. Hamada, M. Sakatani, C. Kobayashi, M. Nishioka, and S. Yamamoto. 1997. CT findings during phase of accelerated deterioration in patients with idiopathic pulmonary fibrosis. *Am. J. Roentgenol.* 168: 79–83.
25. Yao-Tseng, C., J. S. Matthew, S. Ugur, T. Ozlem, O. G. Ali, T. Solam, W. Barbara, S. Elisabeth, P. Michael, and J. O. Lloyd. 1997. A testicular antigen aberrantly expressed in human cancers detected by autologous antibody screening. *Proc. Natl. Acad. Sci. USA* 94: 1914–1918.
26. Matsunaga, Y., Y. Usui, and Y. Yoshizawa. 2003. TA-19, a novel protein antigen of *Trichosporon asahii*, in summer-type hypersensitivity pneumonitis. *Am. J. Respir. Crit. Care Med.* 167: 991–998.

27. Capelli, A., M. Lusuardi, S. Carli, and C. F. Donner. 1991. Acid phosphatase (E.C. 3.1.3.2) activity in alveolar macrophages from patients with active sarcoidosis. *Chest* 99: 545–550.
28. Langerak, A. W., R. Beemd, I. L. Wolvers-Tettero, P. P. Boor, E. G. van Lochem, H. Hooijkaas, and J. J. van Dongen. 2001. Molecular and flow cytometric analysis of the Vβ repertoire for clonality assessment in mature TCRαβ T-cell proliferations. *Blood* 98: 165–173.
29. Lefranc, M. P., G. Giudicelli, C. Ginestoux, J. Bodmer, W. Muller, R. Bontrop, M. Lemaitre, A. Malik, V. Barbie, and D. Chaume. 1999. IMGT, the international ImMunoGeneTics database. *Nucleic Acids Res.* 27: 209–212.
30. Rescher, U., V. Goebeler, A. Wibers, and V. Gerke. 2006. Proteolytic cleavage of annexin I by human leukocyte elastase. *Biochim. Biophys. Acta* 1763: 1320–1324.
31. Robinson, C., M. Callow, S. Stevenson, B. W. Robinson, and R. A. Lake. 2001. Private specificities can dominate the humoral response to self-antigens in patients with cryptogenic fibrosing alveolitis. *Respir. Res.* 2: 119–124.
32. Savill, J., V. Fadok, P. Henson, and C. Haslett. 1993. Phagocyte recognition of cells undergoing apoptosis. *Immunol. Today* 14: 131–136.
33. Casciola-Rosen, L. A., G. Anhalt, and A. Rosen. 1994. Autoantigens targeted in systemic lupus erythematosus are clustered in two populations of surface structures on apoptotic keratinocytes. *J. Exp. Med.* 179: 1317–1330.
34. Mevorach, D., J. L. Zhou, X. Song, and K. B. Elkon. 1998. Systemic exposure to irradiated apoptotic cells induces autoantibody production. *J. Exp. Med.* 188: 387–392.
35. Gulati, T. D., K. B. Elkon, A. E. Ghanavi, and J. G. Krueger. 1992. Enhanced membrane binding of autoantibodies to cultured keratinocytes of systemic erythematosus patients after ultraviolet B/ultraviolet A irradiation. *J. Clin. Invest.* 90: 1067–1076.
36. Geasler, T. J., M. Hottelet, and C. Zhang. 2001. Monoclonal antibodies derived from BALB/c mice immunized with apoptotic Jurkat T cells recognize known autoantigens. *J. Autoimmun.* 16: 59–69.
37. Wang, L., J. F. Scabilloni, J. M. Antonini, Y. Rojanasakul, V. Castranova, and R. R. Mercer. 2006. Induction of secondary apoptosis, inflammation, and lung fibrosis after intratracheal instillation of apoptotic cells in rats. *Am. J. Physiol.* 290: L695–L702.
38. Raynal, P., and H. B. Pollard. 1994. Annexins: the problem of assessing the biological role for a gene family of multifunctional calcium- and phospholipids-binding proteins. *Biochim. Biophys. Acta* 1197: 63–93.
39. Nagase, T., N. Uozumi, S. Ishii, Y. Kita, H. Yamamoto, E. Ohga, Y. Ouchi, and T. Shimizu. 2002. A pivotal role of cytosolic phospholipase A_2 arachidonyl trifluoromethyl ketone, attenuates LPS-induced lung injury in mice. *Nat. Med.* 8: 480–484.
40. Hayes, M. J., and S. E. Moss. 2004. Annexins and disease. *Biochem. Biophys. Res. Commun.* 322: 1166–1170.
41. Walther, A., K. Riehemann, and V. Gerke. 2000. A novel ligand of the formyl peptide receptor: annexin I regulates neutrophil extravasation by interacting with the FPR. *Mol. Cell.* 5: 831–840.
42. Xu, Q., and J. C. Reed. 1998. Bax-inhibitor-1, a mammalian apoptosis suppressor identified by functional screening in yeast. *Mol. Cell.* 1: 337–346.
43. Chae, H. J., H. R. Kim, C. Xu, B. Bailly-Maitre, M. Krajewska, S. Krajewski, S. Banares, J. Cui, M. Digicaylioglu, N. Ke, et al. 2004. BI-1 regulates an apoptosis pathway linked to endoplasmic reticulum stress. *Mol. Cell.* 15: 355–366.
44. Kuwano, K., N. Hagimoto, T. Maeyama, M. Fujita, M. Yoshimi, I. Inoshima, N. Nakashima, N. Hamada, K. Watanabe, and N. Hara. 2002. Mitochondria-mediated apoptosis of lung epithelial cells in idiopathic interstitial pneumonias. *Lab. Invest.* 82: 1695–1706.
45. Sturniolo, T., E. Bono, J. Ding, L. Raddrizzani, O. Tuereci, U. Sahin, M. Braxenthaler, F. Gallazzi, M. P. Protti, F. Sinigalia, and J. Hammer. 1999. Generation of tissue-specific and promiscuous HLA ligand databases using DNA microarrays and virtual HLA class II matrices. *Nat. Biotechnol.* 17: 555–561.
46. Hammer, J., T. Sturniolo, and F. Sinigaglia. 1997. HLA class II peptide binding specificity and autoimmunity. *Adv. Immunol.* 66: 67–100.
47. Tsao, F. H., K. C. Meyer, X. Chen, N. S. Rosenthal, and J. Hu. 1998. Degradation of annexin I in bronchoalveolar lavage fluid from patients with cystic fibrosis. *Am. J. Respir. Cell Mol. Biol.* 18: 120–128.
48. Chung, Y. W., H. Y. Oh, J. Y. Kim, J. H. Kim, and I. Y. Kim. 2004. Allergen-induced proteolytic cleavage of annexin-1 and activation of cytosolic phospholipase A_2 in the lungs of a mouse model of asthma. *Proteomics* 4: 3328–3334.

Journal of proteome research

Article

Identification of Predictive Biomarkers for Response to Trastuzumab Using Plasma FUCA Activity and N-Glycan Identified by MALDI-TOF-MS

Kazuko Matsumoto, Chikako Shimizu, Tokuzo Arao, Masashi Andoh, Noriyuki Katsumata, Tsutomu Kohno, Kan Yonemori, Fumiaki Koizumi, Hideyuki Yokote, Kenjiro Aogi, Kenji Tamura, Kazuto Nishio, and Yasuhiro Fujiwara

J. Proteome Res., **Article ASAP** • DOI: 10.1021/pr800655p

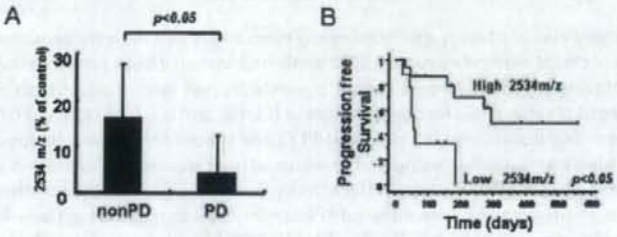

More About This Article

Additional resources and features associated with this article are available within the HTML version:

- Supporting Information
- Access to high resolution figures
- Links to articles and content related to this article
- Copyright permission to reproduce figures and/or text from this article

View the Full Text HTML